

# Fluorescence sensors for imaging membrane lipid domains and cholesterol

Running head: Sensor-mediated visualization of membrane domains

 The corrections made in this section will be reviewed and approved by a journal production editor.

 Francisco J. Barrantes\* [francisco\\_barrantes@uca.edu.ar](mailto:francisco_barrantes@uca.edu.ar)

Biomedical Research Institute (BIOMED), Catholic University of Argentina (UCA)–National Scientific and Technical Research Council (CONICET), Buenos Aires, Argentina

\*Corresponding author:

---

## Abstract

Lipid membrane domains are supramolecular lateral heterogeneities of biological membranes. Of nanoscopic dimensions, they constitute specialized hubs used by the cell as transient signaling platforms for a great variety of biologically important mechanisms. Their property to form and dissolve in the bulk lipid bilayer endow them with the ability to engage in highly dynamic processes, and temporarily recruit subpopulations of membrane proteins in reduced nanometric compartments that can coalesce to form larger mesoscale assemblies. Cholesterol is an essential component of these lipid domains; its unique molecular structure is suitable for interacting intricately with crevices and cavities of transmembrane protein surfaces through its rough  $\beta$  face while “talking” to fatty acid acyl chains of glycerophospholipids and sphingolipids via its smooth  $\alpha$  face.

Progress in the field of membrane domains has been closely associated with innovative improvements in fluorescence microscopy and new fluorescence sensors. These advances enabled the exploration of the biophysical properties of lipids and their supramolecular platforms. Here I review the rationale behind the use of biosensors over the last few decades and their contributions towards elucidation of the in-plane and transbilayer topography of cholesterol-enriched lipid domains and their molecular constituents. The challenges introduced by super-resolution optical microscopy are discussed, as well as possible scenarios for future developments in the field, including virtual (“no staining”) staining.

---

## Keywords:

No keywords are available

## 1 Introduction

For many years, the unavailability of appropriate sensors precluded the unambiguous determination of the physical state of biological membranes and the possibility of unraveling the contribution of individual lipid species to the suspected heterogeneous distribution of lipids across the bilayer. Parallel developments of cell biological, biochemical and biophysical approaches in this area of research have produced steady advances in the membrane biology field, narrowing down the number of unknowns while posing fascinating new questions about the organization and dynamics of membranes.

From a historical perspective, interest in understanding the properties of lipids in membranes and micelles gained momentum in the early 1970s when various physical approaches converged to characterize lipid phases and polymorphisms using small-angle X-ray techniques pioneered by Vittorio Luzzati and coworkers in Gif-sur-Yvette (Luzzati, Gulik-Krzywicki, Rivas, Reiss-Husson, & Rand, 1968; Luzzati & Husson, 1962), nuclear magnetic resonance by Dennis Chapman and coworkers (Cater, Chapman, Hawes, & Saville, 1974) and electron spin resonance by Marsh and his group (Marsh, 1974). Initial attempts to use fluorescent probes to study membrane fragments from mitochondria employed the classical fluorochrome 8-anilino-1-naphthalene-sulfonic acid (ANS) introduced by Gregorio Weber in studies on protein conformation (Weber, 1952; Weber & Laurence, 1954) to gain information on the energy state of this organelle (Azzi, Chance, Radda, & Lee, 1969). Early applications of fluorescence techniques to the study of biomembranes can be traced back to pioneer studies in Gregorio Weber's laboratory. These studies were an extension of Weber's more general interest in fluorescence polarization theory and applications. The fluorescent probes perylene and 2-methylantracene were incorporated into synthetic micelles to apply Perrin's polarization equations in an early investigation of microviscosity and order in the hydrocarbon region of micelles (Shinitzky, Dianoux, Gitler, & Weber, 1971). Subsequent studies applied these techniques to study thermotropic phase transitions and the effect of cholesterol on the microviscosity and order of phospholipid-containing synthetic membranes (Cogan, Shinitzky, Weber, & Nishida, 1973; Jacobson & Wobschall, 1974). See Chapter 6 in this Volume for a thorough analysis of methods to investigate liquid-liquid phase transitions.

The topic of lipid domains in membranes is intimately associated with the physicochemical properties of cholesterol, owing to the crucial involvement of this neutral lipid in the formation of such specialized domains together with phosphoglycerolipids and sphingolipids with saturated acyl chains. As will become apparent throughout this review, efforts devoted to exploring the multiple properties of cholesterol in a lipid bilayer have also brought new insights in the area of lipid domains and, reciprocally, the tools developed for investigating domains have helped to unravel new properties of cholesterol.

Physicochemical studies on artificial membrane-mimetic systems consisting of phospholipid and cholesterol have documented the generation of separated and coexisting liquid-liquid phases, one rich in cholesterol and saturated lipids, the liquid-ordered phase (Lo), and the more "fluid" liquid-disordered (Ld) phase, enriched in unsaturated acyl chain lipids. These physicochemical properties of membrane lipids gave rise to the concept of lipid "rafts," a hypothesis of great gravitation in membrane biology for the last four decades (Ahmed, Brown, & London, 1997; Jacobson, Mouritsen, & Anderson, 2007; Simons & Ikonen, 1997). According to this concept, principles similar to those operating in the above-mentioned complex lipid mixtures *in vitro* are responsible for the self-organization of separate domains in natural cell membranes, generating lateral heterogeneities, i.e. laterally segregated regions or domains, in the lipid bilayer. In this scenario, the "raft" domains display the physicochemical characteristics of liquid-ordered (Lo) gels (Samsonov, Mihalyov, & Cohen, 2001) whereas the remainder of the lipids are purportedly in a liquid-disordered (Ld) phase. Because of their postulated highly dynamic nature and small lateral dimensions (10–200 nm) (Mayor & Rao, 2004; Sezgin, Levental, Mayor, & Eggeling, 2017) raft domains have been elusive to characterize. The interest in directly visualizing these domains has increasingly attracted membrane biologists because of the important functional properties attributed to these distinct regions of the membrane, especially in the realm of signal transduction, constituting hubs where certain membrane proteins are sorted out and platforms for a variety of signaling mechanisms.

Cholesterol remains the quintessential component of these liquid-ordered lipid domains. Unesterified cholesterol synthesized *de novo* in the endoplasmic reticulum (Maxfield & Tabas, 2005; Yeagle, 1989) or derived from external sources via low-density lipoprotein (LDL) receptor-mediated internalization (Brown & Goldstein, 1984) resides mostly (~ 90%) in the plasma membrane, where it can account for up to half of the total lipid content, depending on the cell type (Lange, Swaisgood, Ramos, & Steck, 1989; Lange, Ye, & Steck, 2004). However, only a small fraction of cholesterol (~ 15% of plasmalemmal lipids) termed "chemically active" cholesterol (Das, Brown, Anderson, Goldstein, & Radhakrishnan, 2014) is accessible for transport; the great majority of cell-surface cholesterol is in the form of complexes with phospholipids and SMs (also known as "chemically inactive" cholesterol) (Lange et al., 2004; Radhakrishnan, Anderson, & McConnell, 2000; Radhakrishnan & McConnell, 1999, 2000) and as such inaccessible for intracellular transport. Studies comparing the transport of newly synthesized cholesterol with that of viruses upon temperature arrest led to the conclusion that cholesterol is transported from the endoplasmic reticulum to the plasmalemma primarily via a non-vesicular process, independently of the classical exocytic (ER → Golgi → plasma membrane) trafficking route (Heino et al., 2000; Urbani & Simoni, 1990).

Early electron microscope studies using freeze-fracture cytochemistry (reviewed in [Severs & Robenek, 1983](#)) were probably among the first experimental data to trigger new ideas on the topography of membranes and the concept of cholesterol-rich Lo raft domains that has been so influential over the last 3 decades. The need to experimentally test these theories initially led to the use of biochemical methods combining detergent extraction with differential centrifugation. This indirect approach was and still is open to criticism due to its artifact-prone nature. New approaches have been introduced in recent years to avoid these artifacts. For instance, the observation that bilayer nanodisks formed by phospholipids and the amphiphilic styrene maleic anhydride (SMA) copolymer preserve the functional and structural integrity of  $\alpha$ -helical and  $\beta$ -barrel transmembrane proteins ([Knowles et al., 2009](#)) has made it possible to directly extract discrete patches of nanoscale dimensions ( $\sim 10$  nm) containing proteins with their surrounding lipid environment from the membrane without the use of detergents ([Jamshad et al., 2011](#)). Despite initial concerns similar to those raised against the Triton X-100/centrifugation assays (e.g. whether lipids exchanged with the rest of the bilayer and simply co-purified with the separated proteins ([Cuevas Arenas et al., 2017](#))), these nanotechnology-based detergent-free methods for the extraction of membrane proteins with their vicinal lipid milieu via SMA-lipid particles (SMALPs) have more recently been validated in prokaryotic ([Teo et al., 2019](#)) and eukaryotic membranes like the retinal rod disk membranes ([Sander et al., 2021](#)).

The difficulty of using biochemical methods to test the occurrence of lipid domains in cells gave impetus to the development of fluorescent membrane sensors and in particular cholesterol probes aimed at identifying and characterizing these structures in situ, i.e. without destroying the integrity of the membrane and introducing the minimum possible structural modifications. As early as 1972 X-ray diffraction studies were conducted on phospholipid bilayers with incorporated ANS, 12-(9-anthroyl)-stearic acid and *N*-octadecyl-naphthyl-2-amine 6-sulfonic acid to assess the location of these fluorescent molecules and the degree of perturbation they might introduce into the system ([Lesslauer, Cain, & Blasie, 1972](#)).

As discussed in this review, the design and synthesis of several organic compounds with appropriate fluorescence properties, the introduction of intrinsically fluorescent sterols like dehydroergosterol and cholestanetriol in combination with extracellular quenchers, and the discovery of fungal or bacterial toxins like filipin or perfringolysin O provided the tools to explore several hitherto unknown properties of cholesterol and learn about lipid domains in membranes, the subject of this review. I address visualization of lipid domains in situ, sensing transbilayer asymmetry and sensing membrane polarity. Finally, I discuss the new requirements imposed by the introduction of superresolution optical microscopy approaches, ending by describing possible future scenarios and developments in this field, including virtual (“no staining”) staining.

## 2 Fluorescent sensors for imaging lipid domains in situ

The application of fluorescence microscopy in the field of membrane biology has a long and successful tradition, which evolved hand in hand with the development of appropriate sensors (for reviews see [Demchenko, Mely, Duportail, & Klymchenko, 2009](#); [Epanand, Kraayenhof, Sterk, Sang, & Epanand, 1996](#)). Synthetic lipid membranes have provided useful model platforms to investigate several physicochemical properties of their counterpart natural biomembranes. One of the most extensively studied properties is the phase behavior exhibited when liquid–liquid phases coexist in the bilayer. This phenomenon is observed when phospholipids with saturated acyl chains and sterols condense to form a liquid-ordered (Lo) phase, which separates from a liquid-disordered (Ld) phase composed predominantly of lipids with unsaturated acyl chains ([Bagatolli, 2006](#); [Dietrich et al., 2001](#); [Kahya, Scherfeld, Bacia, Poolman, & Schwille, 2003](#); [Kahya, Scherfeld, & Schwille, 2005](#); [Korlach, Schwille, Webb, & Feigenson, 1999](#); [Veatch & Keller, 2002, 2003a, 2003b, 2005](#)). Attempts to correlate the phase behavior of lipids in model systems at equilibrium with the behavior of lipids in natural membranes has often made use of fluorescence techniques (see e.g. [Bacia, Scherfeld, Kahya, & Schwille, 2004](#); [Baumgart et al., 2007](#)). Giant vesicles derived from plasma membranes by chemically-induced blebbing of the plasma membrane of cultured cells have also been employed as a model to study phase segregation in membrane bilayers ([Baumgart et al., 2007](#)).

Sterol structure influences liquid-ordered domain formation. The behavior of different sterols was found to be similar in symmetric (mixtures of sphingomyelin (SM), 1,2-dioleoyl-sn-glycero-3-phosphocholine (DOPC) and cholesterol), and asymmetric vesicles (in which SM was introduced into the outer leaflet). Cholesterol and 7-dehydrocholesterol strongly stabilized ordered domains in symmetric model membranes, while lanosterol, epicholesterol and desmosterol produced a moderate level of stabilization and 4-cholesten-3-one did not stabilize Lo domains at all ([St. Clair & London, 2019](#)).

The ability to support Lo domains decreased in the order 7-DHC > cholesterol > desmosterol > lanosterol > epicholesterol > 4-cholesten-3-one. Endocytosis levels and bacterial uptake are even more closely correlated with the ability of sterols to form ordered domains than previously thought, and do not necessarily require sterols to have a  $3\beta$ -OH group (St. Clair & London, 2019).

The ideal condition for imaging lipid domains in cells or membrane model systems with fluorescence microscopy is that the fluorescent sensor exhibit a preferential partitioning for one type of domain only, or that it exhibit some spectroscopic property that differentiates between the two domains, such as a marked shift in the fluorescence emission. A systematic search for such sensors shows that most of the probes used for this purpose partition preferentially into the liquid-disordered phase and few do so in cholesterol-rich Lo domains.

## 2.1 Carbocyanines

Carbocyanines are voltage-sensitive compounds introduced in the early 1980s, originally for application in the Neurosciences (optical recordings of membrane potential) (see review in Honig & Hume, 1989) and gradually used more widely as neuronal tracers and for the study of membrane fluidity in a variety of cells and tissues. Carbocyanine dyes share two conjugated planar ring structures substituted at a single position with isopropyl, oxygen or sulfur, giving rise to the DiI (1,1'-dioctadecyl-3,3,3',3'-tetramethylindocarbocyanine perchlorate), diO (3,3'-dioctadecyloxacarbocyanine) and diS families of fluorescent probes. One of the most used of these probes is diI-C18 (1,1'-dioctadecyl-3,3,3',3'-tetramethylindo-carbocyanine perchlorate). The length of the two acyl chains (e.g. 18 C atoms each in the case of DiI-C18) determines the affinity of the compound for the hydrophobic region of the membrane. Carbocyanines with short alkyl chains partition between the water phase and the membrane in a membrane potential-dependent manner, whereas the long-chain carbocyanine dyes are readily inserted into membrane bilayers.

In the field of physicochemistry of membranes, carbocyanines have been assayed in various model systems. The two carbocyanine dyes DiI16 and DiI18 (1,1'-dioctadecyl-3,3,3',3'-tetramethylindocarbocyanine perchlorate) have found application as sensors of membrane domains. For instance, giant unilamellar vesicles (GUVs) composed of DOPC/BSM/cholesterol (2:2:1) display separation into a liquid-disordered and a liquid-ordered phase at room temperature, and incorporation of the probes Fast DiO, Fast DiI and DiD-C18 make apparent the heterogeneous fluorescence distribution of the two coexisting phases (Baumgarten, Makielski, & Fozzard, 1991; Sezgin et al., 2012). In some cases the bulkiness of the fluorophore moiety of the probes results in mutual interferences. For instance, the partitioning of DiIC18 interferes with that of the phospholipid analogue BODIPY-PC [2-(4,4-difluoro-5,7-dimethyl-4-bora-3a,4a-diaza-s-indacene-3-pentanoyl)-1-hexa-decanoyl-sn-glycero-3-phosphocholine].

The long-chain carbocyanine probes of the DiI family are highly lipophilic, and as such are excellent markers of membranes for cell biology experiments requiring good long-term viability of the cells, strong emission, homogeneous labeling, and compatibility with aldehyde fixation, requirements fulfilled by these sensors. These properties have been successfully exploited for the cytochemical identification of neurons and retrograde labelling upon injection of the dye into embryonic preganglionic neurons (Godement, Vanselow, Thanos, & Bonhoeffer, 1987).

## 2.2 DPH diphenylhexatriene (DPH)

1,6-Diphenyl-1,3,5-hexatriene (DPH) is a linear molecule with two phenyl groups at the extremes of its linear hydrocarbon chain. It is barely soluble in aqueous media and highly fluorescent in organic solvents or in membranes. Among the earliest applications of the probe was the measurement of steady-state fluorescence anisotropy of DPH in lymphocyte and lymphoma cells (Shinitzky & Inbar, 1976) in conjunction with that of hydroxy-coumarin and trans-parinaric acid to study the effects of cholesterol and cholest-4-en-3-one on the thermotropic behavior of dipalmitoyl-phosphatidylcholine bilayers. The authors demonstrated the broadening of the gel-to-liquid phase transition of the phospholipid by the sterols and one of the first indications of cholesterol-rich domains in bilayers (Ben-Yashar & Barenholz, 1989). The degree of polarization of DPH increases with increasing cholesterol content (Wharton, De Martinez, & Green, 1980). The position and relative orientation of a series of DPH derivatives in the membrane was established using nitroxide spin-labeled lipids as quenchers and parallax analysis (Kaiser & London, 1998). The cationic derivative of DPH, TMA-DPH (1-(4-trimethylammonium-phenyl)-6-phenyl-1,3,5-hexatriene), is more soluble than its parental compound and its polar moiety positions it in a shallower (0.3–0.4 nm) location in membrane bilayers, establishing electrostatic interactions with electronegative lipid atoms (do Canto et al., 2016). TMA-DPH has been used in studies on endocytic processes (Illinger, Duportail, Poirel-Morales, Gerard, & Kuhry, 1995; Illinger, Italiano, Beck,

Waltzinger, & Kuhry, 1993; Illinger, Poindron, & Kuhry, 1991). Fluorescence lifetime measurement of TMA-DPH has mostly been used as a sensor of the exofacial membrane leaflet using either fluorescence anisotropy or fluorescence lifetime measurements (Chazotte, 2011). A phosphatidylcholine derivative of DPH senses slightly different regions of the plasma membrane than do DPH or TMA-DPH, but the probe has not had extensive use in membrane studies (Ferretti, Tangorra, Zolese, & Curatola, 1993; Tangorra, Ferretti, Zolese, & Curatola, 1994).

Steroids exert influence on Lo domain formation and stabilization, and on the extension of the ordered assemblies. Combining two independent biophysical methods (steady-state anisotropy measurements of DPH with temperature-dependent fluorescence quenching by a nitroxide spin-labeled phosphatidylcholine (PC) (12-SLPC)) we studied the effect of steroid structure on the above properties of liquid-ordered domains. Lo domain-promoting steroids were found to exhibit a small polar group at position C3, an isooctyl side chain bond at C17, absence of carbons attached to C23 (i.e., C24–C27), and absence of polar groups in the fused rings, with the exception of substitutions at position C3 in the A ring (Wenz & Barrantes, 2003).

### 2.3 Parinaric acid

cis-Parinaric acid (cis-trans-trans-cis-9,11,13, 15-octadecatetraenoic acid or 9Z,11E,13E,15Z-octadecatetraenoic acid), discovered by Tsujimoto and Koyanagi in 1933, is a naturally occurring conjugated polyunsaturated fatty acid found in the seeds of the Makita tree, indigenous to Fiji. It contains an unusual conjugated tetraene which confers fluorescence to the fatty acid. Upon excitation at 320 nm it emits at 432 nm. *cis*-parinaric acid has been employed for the measurement of lipid enzyme activities (phospholipase, lipase), and as an indicator of lipid peroxidation. The polarization of fluorescence and the lifetime of *cis*-parinaric acid have been exploited to learn about the physical status of biomembranes (Calafut, Dix, & Verkman, 1989; Ruggiero & Hudson, 1989a, 1989b). The ligand binding site for fatty acids and cholesterol carrier proteins (Schroeder, Myers-Payne, Billheimer, & Wood, 1995; Stolowich et al., 1997) as well as its location in the membrane bilayer (Castanho, Prieto, & Acuña, 1996) and the role of cholesterol in liquid-ordered domains of caveolae (Gallegos, McIntosh, Atshaves, & Schroeder, 2004) have been investigated using this sensor.

### 2.4 NBD-derivatives

Adducts of the relatively small fluorophore 4-chloro-7-nitrobenzofurazan (NBD) have been used to label many different biological molecules, and lipids in particular [Instruction: delete full stop and relace by a comma, and replace capital F by small f, to read:

... and lipids in particular, for instance....], **F**for instance fatty acids like the saturated octadecanoic acid derivative NBD-stearic acid [12-(*N*-methyl)-*N*-[(7-nitrobenz-2-oxa-1,3-diazol-4-yl)amino]-octadecanoic acid]. Phosphoglycerolipids such as PE have been tagged covalently with the fluorophore (NBD-DPPE [1,2-dipalmitoyl-sn-glycero-3-phosphoethanolamine-*N*-(7-nitro-2-1,3-benzoxadiazol-4-yl)]), and this fluorescent lipid has been shown to be a sensor of the liquid-ordered phase together with the more bulky planar probe NAP (naphtho[2,3-*a*]pyrene) (Juhász, Davis, & Sharom, 2010).

The so-called red-edge excitation shift or REES is observed with polar fluorophores in motionally restricted, viscous media, or in condensed phases where the dipolar relaxation time for the solvent shell around the fluorophore is comparable to or longer than its fluorescence lifetime (Chattopadhyay, 2003). NBD-tagged lipids show the REES effect, shifting their maximum fluorescence emission toward higher wavelengths, owing to the shift in the excitation wavelength toward the red edge of the absorption band. The REES effect was originally interpreted as stemming from the slow rates of solvent relaxation (reorientation) around the fluorophore in its excited state (Chattopadhyay, 2003), i.e. from mobility constraints of the solvent molecules surrounding the fluorescent sensor. Other authors considered that the REES effect is independent of temperature and cholesterol content, and therefore insensitive to water relaxation phenomena, attributing the phenomenon to the anomalous transverse location of the probe in the membrane (Amaro, Filipe, Prates Ramalho, Hof, & Loura, 2016). The peculiar orientation of the nitro group determines the fluorescence lifetime of NBD in the membrane (Filipe, Pokorná, Hof, Amaro, & Loura, 2019). The REES effect has been exploited to determine the topology of the membrane-bound colicin E1 channel in the bilayer, utilizing the emission of tryptophan residues (Tory & Merrill, 2002). Chattopadhyay and coworkers have made extensive use of REES of NBD-tagged phospholipids, which were reported to undergo a noticeable red-edge shift upon incorporation into artificial bilayers (Chattopadhyay & Mukherjee, 1993; Mukherjee & Chattopadhyay, 1995; Raghuraman & Chattopadhyay, 2004).

## 2.5 FITC-chitosan derivatives


Fluorescein-isothiocyanate (FITC)-labeled glycol chitosan molecules have been reported to label lipid-ordered domains in model or cell membranes (Jiang et al., 2016). Since the FITC-labeled glycol chitosan molecules do not completely insert into the lipid bilayer but interact presumably via attractive electrostatic interactions and/or hydrophobic interactions with the ordered domain lipids, it is considered that they do not disturb the membrane organization. This family of probes are non-permeant indirect reporter groups of cholesterol localization in lipid-ordered domains in living cells.

## 2.6 Polyethylene-glycol-derivatized cholesterol

Another membrane-impermeable sensor of cholesterol-rich ordered lipid domains is the fluorescent derivative of polyethylene oxide (poly(ethyleneglycol)cholesteryl ether (fPEG-cholesterol) introduced by Kobayashi and coworkers (Sato et al., 2004). The membrane impermeability of fPEG-Chol make it a sensor of liquid-ordered lipid microdomains located in the outer plasma membrane leaflet (Sato et al., 2004). fPEG-cholesterol has been used alone or in conjunction with the sphingomyelin-binding protein lysenin (Hullin-Matsuda & Kobayashi, 2007) to label cholesterol-rich lipid domains in living cells (Hullin-Matsuda & Kobayashi, 2007). fPEG-cholesterol has also been used to follow the endocytic internalization of the nicotinic receptor protein and cholesterol (Kamerbeek et al., 2013).

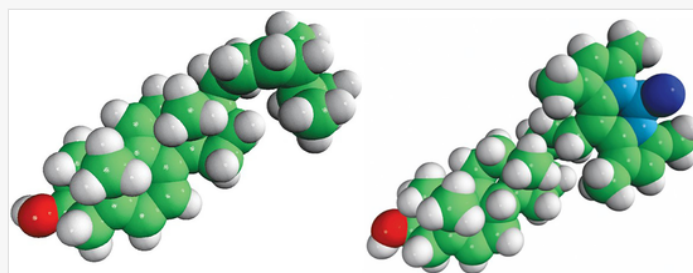
## 2.7 Intrinsically fluorescent cholesterol analogues dehydroergosterol and cholestanetriol

Two polyene sterols with a high degree of structural similarity to cholesterol have been extensively used in biophysical and cell biological studies of membranes addressing the location and trafficking of cholesterol in cells. These are dehydroergosterol ((DHE,  $\Delta^{5,7,9(11),22}$ -ergostatetraen-3 $\beta$ -ol) and cholestanetriol (5- $\beta$ -cholestane-3- $\alpha$ ,7- $\alpha$ , 12- $\alpha$ -triol, CTL) (Fig. 1).

 Images are optimised for fast web viewing. Click on the image to view the original version.

alt-text: Fig. 1

Fig. 1



Molecular models depicting one of the smallest cholesterol fluorescent sensors. Left: the naturally fluorescent cholesterol analogue dehydroergosterol (ergosta-5,7,9(11),22-tetraen-3 $\beta$ -ol, DHE), and right: the bulkier TopFluo-cholesterol (23-(dipyrometheneboron difluoride)-24-norcholesterol).

Images provided by Avanti Polar Lipids.

DHE is a fluorescent derivative of ergosterol, a natural sterol found in yeasts such as *Saccharomyces cerevisiae*. CTL is the closest structural analogue of cholesterol, differing only in having two additional double bonds in the planar ring system while its aliphatic side chain is identical to that of cholesterol. The three conjugated double bonds in the sterol backbone provide CTL with intrinsic fluorescence. Shared with DHE, this advantageous property is counterbalanced by the fact that absorption and emission occur in the UV region of the spectrum, thus reducing their usefulness for imaging live cells, particularly with conventional wide-field fluorescence microscopy, because of its damaging effects on cell viability (Schroeder et al., 2005). In addition, DHE has a high photobleaching rate. Nonetheless, DHE has been successfully combined with wide-field microscopy using quartz optics to study the cellular topography and traffic of this cholesterol analogue ((Hao et al., 2002; Hao, Mukherjee, & Maxfield, 2001; Mondal, Mesmin, Mukherjee, & Maxfield, 2009; Mukherjee, Zha, Tabas, & Maxfield, 1998; Wüstner, Herrmann, Hao, & Maxfield, 2002) and see

review in (Maxfield & Wüstner, 2012)). The quartz optics can be bypassed by the use of multiphoton laser excitation (McIntosh et al., 2007; McIntosh et al., 2008).

Biophysical studies have shown that DHE induces the formation of liquid-ordered domains in bilayers and giant unilamellar vesicles (GUVs) containing phospholipids and cholesterol (Garvik, Benediktson, Simonsen, Ipsen, & Wüstner, 2009). Contrary to expectations, the probe does not exhibit red-edge excitation shift in model membranes, irrespective of the phase state of the membrane, an observation that has been interpreted as implying the probe's lack of environmental sensitivity, attributable to the very small change in its dipole moment upon excitation (Chattopadhyay, Biswas, Rukmini, Saha, & Samanta, 2021).

Unlike DHE and ergosterol, CTL exerts an ordering effect on the fatty acid acyl chains of the hydrophobic region of the bilayer (Solanko, Modzel, Solanko, & Wüstner, 2015). Both DHE and CTL induce ordering of phospholipid bilayers composed of palmitoyl-oleoyl-phosphatidylcholine or palmitoyl-oleoyl-phosphatidylcholine/cholesterol, although the degree of order is lower than that induced by cholesterol itself (Robalo, do Canto, Carvalho, Ramalho, & Loura, 2013).

DHE and CTL exhibit small differences in metabolism in comparison to cholesterol. For instance, DHE is unable to bind to several proteins involved in cholesterol metabolism in the ER and activate sterol regulatory element-binding protein 2 (Mesmin et al., 2011). Uptake and esterification of DHE by non-lipoprotein pathways is lower than that of cholesterol. DHE is also a less efficient substrate of acyl-CoA:cholesterol acyltransferase than cholesterol (Liu, Chang, Westover, Covey, & Chang, 2005). The applications of DHE or CTL in fluorescence microscopy of living cells are limited by their low quantum yield, high photobleaching rate, and their absorption and emission bands in the UV region of the spectrum, overlapping with the UV absorption of essentially all protein constituents of the cell, with inherent deleterious effects when irradiated in this spectral region using wide-field microscopy.

## 2.8 Sphingomyelin sensors

Sphingophosphorylcholine and a fatty acid coupled to a fluorophore like nitrobenzoxadiazole (NBD) or boron dipyrromethene difluoride (BODIPY) have been used as sphingomyelin sensors, and, indirectly, of ordered lipid domains in membranes. Short-chain fatty acid acyl moieties in these sensors favor partition of the probe into liquid-disordered bulk phase lipid domains, although natural sphingomyelins show preference for liquid-ordered domains (Kinoshita et al., 2017; Kishimoto, Ishitsuka, & Kobayashi, 2016). The water-soluble quencher dithionite selectively quenched NBD-labeled sphingomyelin in the outer leaflet of the membrane (McIntyre & Sleight, 1991). The pore-forming sphingomyelin-binding protein lysenin has been used to study the localization of the lipid in cells (Carquin et al., 2014) and discloses the occurrence of sphingomyelin-rich domains larger than 100 nm in diameter in the inner leaflet of the plasma membranes of human skin fibroblasts and neutrophils (Murate et al., 2015). A non-toxic mushroom protein termed Nakanori that specifically binds to a complex of sphingomyelin and cholesterol has been used to label cell-surface ordered domains and also lipid domains that colocalized with inner leaflet small GTPase H-Ras, but not K-Ras (Makino et al., 2017). Nakanori was also employed to study the altered distribution of cholesterol and sphingomyelin in Niemann-Pick type C fibroblasts (Makino et al., 2017).

## 3 Sensing transbilayer topography of lipids, cholesterol, and lipid domains

The distribution of lipid components in the axis perpendicular to the plane of the membrane bilayer has interested biophysicists for decades. The transbilayer topography of lipids across the membrane bilayer, including that of cholesterol, is important for cell homeostasis and is hence under tight metabolic control. The cell maintains higher concentrations of PCs and SMs in the outer membrane leaflet, whereas phosphatidylethanolamine (PE), phosphatidylserine (PS) and phosphatidylinositol (PI) phosphoglycerolipids predominate in the inner leaflet (Kobayashi & Menon, 2018; van Meer, Voelker, & Feigenson, 2008). This varies between membranes: phosphatidylserine is mainly at the cytoplasmic leaflet in the plasmalemma, whereas it is in the luminal leaflet in the endoplasmic reticulum (Kobayashi & Menon, 2018). Asymmetric distribution of lipids obviously obeys functional requirements, particularly in the plasma membrane, which separates two totally different universes. Maintaining asymmetrical topography requires active processes and energy expenditure: the free energy barrier associated with the spontaneous translocation of a charged lipid from one face of the membrane to the other is high.

The asymmetry does not pertain exclusively to the phospholipids; lipidomic studies have established that the compositional differences between the two membrane leaflets also includes the degree of unsaturation of the acyl chains and packing, as well as asymmetries in membrane protein shape and translational diffusion. Using enzymatic digestion combined with mass spectroscopy of red blood cells, the distribution of around 400 lipid species could be determined: the inner leaflet of the plasma membrane contains on average two-fold more unsaturated lipids than the exoplasmic leaflet, while the latter is more densely packed and hence less diffusive than the cytoplasmic-facing hemilayer (Lorent et al., 2020).

The distribution of cholesterol across the two leaflets of the plasma membrane is less clear than that of phospholipids; despite its relatively high concentration in plasma membranes the issue remains controversial, with some authors maintaining that cholesterol occurs mostly in the exofacial hemilayer and others sustaining the opposite view (Giang & Schick, 2016; Steck & Lange, 2018; van Meer, 2011). Cholesterol transbilayer distribution depends on the ATP-dependent P4-ATPases, also termed “flippases,” which actively translocate the aminophospholipids PS and PE to the cytosolic-facing hemilayer, whereas the ATP-binding cassette (ABC) ABCA1 and ABCG1 transporters translocate lipids in the opposite direction as exporters rather than “floppases” ((van Meer, 2011) and see review in (Liu, 2019)). Dysfunction of these transporters is known to occur in various diseased conditions like metabolic syndrome, atherosclerosis, cardiovascular disease, cystic fibrosis, retinal degeneration, and cholestasis (Liu, 2019).

A method based on tunable orthogonal cholesterol sensors has been developed to simultaneously quantify cholesterol in the two leaflets of the plasma membrane (Liu et al., 2017). The technique revealed marked transbilayer cholesterol asymmetry in several mammalian cells: cholesterol concentration in the inner leaflet was found to be ~ 12-fold lower than that in the outer leaflet. The asymmetry was maintained by active transport of cholesterol from the inner to the outer leaflet and by its retention at the exofacial leaflet. The increase in the cytoplasmic leaflet cholesterol level was triggered in a stimulus-specific manner -e.g. Wnt signaling activity- leading to the notion that cholesterol serves as a signaling function (Liu et al., 2017). Another bio-orthogonal cholesterol sensor has recently been developed and used in conjunction with super-resolution microscopy to image lipid domains of < 50 nm diameter in the plasmalemma of live cells (Lorizate et al., 2021).

The transbilayer distribution of cholesterol remains controversial, partly because (i) the sterol does not occur in a single pool; (ii) cholesterol does not show an homogeneous in-plane distribution; (iii) it can flip-flop between the two leaflets of the bilayer (Ikonen, 2008); [Instruction: replace comma by semi colon] and (iv) the distribution of the cholesterol pool residing in liquid-ordered lipid domains (“rafts”) is likely to differ from that of the “free” cholesterol pool in the membrane. In fact the original “raft” hypothesis favored the notion that Lo lipid domains occur in the outer, exofacial leaflet of the membrane (Simons & Ikonen, 1997). Ever since this seminal idea, the subject of cholesterol distribution across the bilayer has remained a contentious and methodologically difficult issue in membrane biology (see (Kobayashi & Menon, 2018; Murate et al., 2015; Murate & Kobayashi, 2016) for reviews on current techniques to study membrane asymmetry). Experimentally, the transbilayer topography of cholesterol has been studied in early work using the intrinsic fluorescent analogue DHE in combination with fluorescence quenching with trinitrobenzene sulfonic acid. DHE was preferentially incorporated into the inner, cytoplasmic-facing hemilayer of the plasma membrane of fibroblast (Hale & Schroeder, 1982) and other cell types (Kier, Sweet, Cowlen, & Schroeder, 1986).

Another aspect of membrane asymmetry that remains controversial is whether a cholesterol-rich ordered domain in one bilayer leaflet can induce ordered domain formation in the opposite membrane leaflet; in other words, whether there is a coupling between domains at opposite regions of the membrane hemilayers. Research on this topic has benefited from the use of artificial lipid vesicles (London, 2019). Using asymmetric and symmetric lipid vesicles composed of SM, cholesterol, and either unsaturated dioleoyl PC (DOPC) or 1-palmitoyl 2-oleoyl PC (POPC) the temperature dependence of Lo domain formation was studied using Förster resonance energy transfer (St. Clair, Kakuda, & London, 2020). In cholesterol-containing asymmetric SM + PC outside/PC inside vesicles, the PC-containing inner leaflet destabilized Lo domain formation in the outer leaflet; ordered domain formation was suppressed by asymmetry over the entire temperature range measured (St. Clair et al., 2020). SMs appear to play an important role in inter-leaflet coupling: SM in the outer leaflet appears to induce Lo domains in asymmetric vesicles (Lin & London, 2015) and long-chain SM depletes cholesterol from the cytoplasmic leaflet in asymmetric membranes (Karlsen, Bruhn, Pezeshkian, & Khandelia, 2021). The presence of SMs with long acyl chain (24 C atoms) in the outer leaflet suppresses Lo domains in the plasma membrane of HeLa cells, under which conditions cholesterol is preferentially found in the inner hemilayer (Courtney et al., 2018).



### 3.1 Intrinsically fluorescent cholesterol analogues, dehydroergosterol and cholestatrienol

In the context of transbilayer sidedness, DHE appears to be a reporter of asymmetry since it partitions in a non-homogeneous manner along the axis perpendicular to the plane of the lipid bilayer. Using trinitrobenzene sulfonic acid as quencher, DHE was shown to partition more favorably into the inner leaflet of the plasma membrane in fibroblast (Hale & Schroeder, 1982) and other cell types (Kier et al., 1986).

In terms of the lateral distribution of DHE in the plasma membrane, work by Wüstner showed that DHE colocalized with fluid membrane-preferring phospholipids in the plasmalemma and associated compartments like microvilli, filopodia, nanotubules and membrane blebs induced by F-actin disruption, but not in cholesterol-rich domains (Wüstner, 2007). However, Wüstner's group later reported that DHE preferentially partitioned in the liquid-ordered membrane domains and induced the formation of such domains in supported bilayers and giant unilamellar vesicles (GUVs) made of dipalmitoyl-phosphatidylcholine, dioleoyl-phosphatidylcholine and Chol (Garvik et al., 2009). The ambiguity of these findings thus casts doubt on DHE's characterization as an "ideal" probe.

### 3.2 Filipin

Filipin, together with nystatin and amphotericin B, are antibiotics with primarily antifungal activity and a lower antibacterial activity, exerted by promoting membrane leakage. Filipin is a complex mixture of at least 4 polyene amphipathic macrolides isolated from the mycelium and culture filtrates of *Streptomyces filipinensis*. This organism has found increasing applications in antifungal biotechnology and as a model organism for understanding how butyrolactones control secondary metabolism and antibiotic production (Barreales, Payero, de Pedro, & Aparicio, 2018). The name filipin derives from its biological origin and this, in turn, from its geographical stem. Fig. 1 shows the structure of filipin.

Filipin was used initially to localize cholesterol in histochemical studies (Börnig & Geyer, 1974; Geyer & Börnig, 1975), and in electron microscope studies of freeze-fractured cells to study the relationship between cholesterol and coated pits/endocytic vesicles (Montesano, Vassalli, & Orci, 1981) as well as the topology of cholesterol in the Golgi complex (Orci et al., 1981). The advantages and disadvantages of filipin as a sensor for the localization of cholesterol in membranes, and its use and abuse, were recognized early (Miller, 1984).

Filipin binds free, unesterified cholesterol (Maxfield & Wüstner, 2012). The fact that it does not bind to esterified sterols provides a technical advantage since the lack of esterified cholesterol in lipid droplets improves the signal-to-noise ratio in cellular studies.


The mechanism through which filipin-cholesterol interactions are established is not totally clear. The three main hypotheses summarized by Prieto and coworkers (Castanho, Coutinho, & Prieto, 1992) are: (i) filipin:sterol form planar 1:1 complexes between the two hemilayers of the membrane; (ii) the complex is established at a 1:1 stoichiometry but at the membrane surface, with concomitant disordering of the bilayer, or (iii) the interaction takes place at the exofacial leaflet of the membrane and the deformation of the bilayer occurs due to the increased surface pressure. van Deenen and coworkers were among the first to study filipin with electron microscopy based on the ability of the antibiotic to induce the formation of pits in erythrocyte membranes, and the presumption that these occurred via filipin-cholesterol interactions (Kinsky, Luse, Zopf, Van Deenen, & Haxby, 1967). The fluorescence properties of filipin were exploited some years later to establish the location of cholesterol in sarcoplasmic reticulum membrane vesicles (Drabikowski, Lagwińska, & Sarzala, 1973). These authors measured excitation and emission spectra of filipin in dimethylformamide (exc.: 360 nm; emiss.: 480 nm) and determined the existence of energy transfer between tryptophan residues and filipin. The photophysical properties and topography of filipin in model membrane systems has been studied using fluorescence quenching with nitroxide spin labels (Castanho & Prieto, 1995).

One drawback of filipin is that it requires fixation of the cell, and hence it cannot be employed in dynamic studies with living cells. There are also drawbacks related to the low specificity of filipin, the first being that filipin does not enable the experimentalist to discern whether the identified cholesterol molecules are those originated by de novo synthesis or whether they are incorporated from the blood stream via lipoprotein-mediated mechanisms. The second, more important downside, is that filipin has been reported to recognize ganglioside GM1 and cholesterol with similar affinities (Arthur, Heinecke, & Seyfried, 2011). Despite these drawbacks filipin is still a useful sensor of cholesterol

topography and has played an important role in our understanding of the pathophysiology of Niemann-Pick disease type C, a cholesterol lysosomal storage disease, over the course of more than three decades of research (Pentchev et al., 1985; Saha et al., 2020).

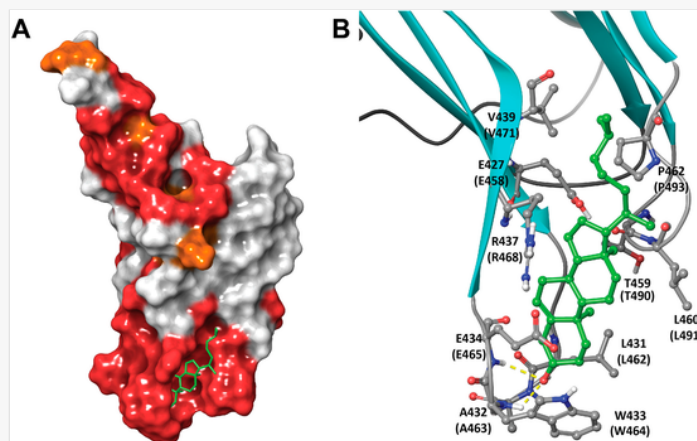
### 3.3 Perfringolysin O

Perfringolysin O, also called theta-toxin, is a cholesterol-binding cytolysin produced by the anaerobic bacterium *Clostridium perfringens*. Cholesterol-dependent cytolysins belong to a family of pore-forming toxins secreted by Gram-positive bacteria. The C-terminus of the cytolysins is also termed domain 4 or simply D4, a region of the protein consisting of two four-stranded  $\beta$ -sheets. Another cytolysin, pneumolysin, is a thiol-activated cytolysin toxin from *Streptococcus pneumoniae* (Saunders, Mitchell, Walker, Andrew, & Boulnois, 1989). Pneumolysin and perfringolysin O share a high degree of homology in their membrane-associating regions (Savinov & Heuck, 2017). Fig. 2 shows the structure of pneumolysin with a cholesterol molecule docked on its surface. The mechanism of action of perfringolysin is relatively well known. It is initiated by the insertion of a large portion of its  $\beta$ -barrel structure into a cholesterol-containing region of the target membrane; the presence of cholesterol is an absolute requirement for this to occur.

 Images are optimised for fast web viewing. Click on the image to view the original version.

alt-text: Fig. 2

Fig. 2



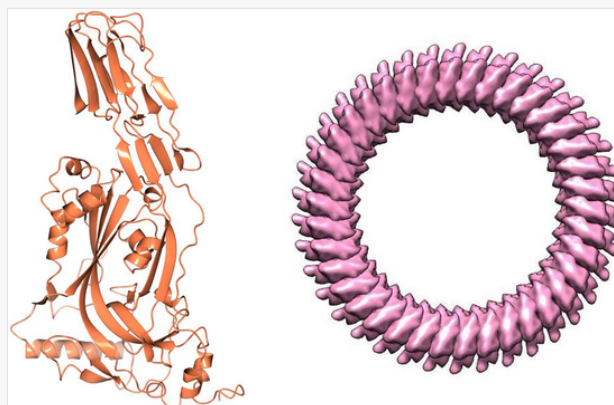
(A) Induced-fitting docking model of the C-terminus (domain 4 or D4) of the cytolysin pneumolysin (surface rendering, where red are identical, orange conserved, and white non-conserved residues in comparison to perfringolysin O analogous residues) with a cholesterol molecule (green wire representation) docked on its surface. The D4 domain is responsible for the cholesterol-dependent membrane binding of cytolysins to cholesterol-containing membranes, thus explaining why this portion of the molecule has been used as a cholesterol sensor. (B) Detail of the cholesterol binding region in pneumolysin predicted by the induced-fitting model. The cholesterol molecule is shown in green ball-and-stick rendering and the pneumolysin undecapeptide as cyan arrows and grey ball-and-stick rendering.

Reproduced from Savinov, S. N., & Heuck, A. P. (2017). Interaction of cholesterol with perfringolysin O: What have we learned from functional analysis? *Toxins (Basel)*, 9(12). doi:10.3390/toxins9120381 under Creative Common CC BY license.

Cytolysin binding to the exofacial hemilayer of cell membranes is the first in a series of steps that may lead to cell death upon infection with *C. perfringens* or *Streptococcus pneumoniae*. Binding is followed by insertion of the toxin, provided cholesterol is present at the cell surface at a certain threshold (40–60%) concentration (Maekawa & Faim, 2015). Cholesterol is necessary and sufficient to trigger perfringolysin O binding to cells, and addition of SM inhibits binding (Flanagan, Tweten, Johnson, & Heuck, 2009). Insertion is followed by dimerization, multimerization, pre-pore formation, and pore formation. At low, sub-lytic concentrations, toxin binding to cells, e.g. mast cells, results in activation, degranulation, and transcriptional activation that leads to cytokine production. At higher toxin concentrations, large pores may be formed by high order multimers of the toxin as shown in Fig. 3, an oligomerization product that may lead to necroptotic cell death. Upon infection with *C. perfringens*, the toxin activates caspase-1 and the inflammasome cascade in the target cell which can progress to gas gangrene (Yamamura et al., 2019).

alt-text: Fig. 3

Fig. 3



Left: Crystal structure of a monomer of perfringolysin O from *C. perfringens* obtained by X-ray crystallography at 2.9 Å resolution (PDB entry: [1MJJ](#)). Right: pore structure of pneumolysin (PDB entry: [2BKL](#), EMDataResource EMD-1107) obtained by fitting the  $\alpha$ -carbon trace of perfringolysin O onto a cryo-EM map of pneumolysin ([Marshall et al., 2015](#)).

Image created using CCP4mg molecular graphics ([McNicholas, S., Potterton, E., Wilson, K. S., & Noble, M. E. \(2011\). Presenting your structures: The CCP4mg molecular-graphics software. Acta Crystallographica. Section D, Biological Crystallography, 67\(Pt. 4\), 386–394. doi:10.1107/s0907444911007281](#)).

Epicholesterol does not interact with perfringolysin O, and its addition to the cell reduces toxin binding ([Flanagan et al., 2009](#)). A study found that the toxin did not discriminate between cholesterol-containing liquid-ordered domains and coprostanol-containing disordered lipid domains ([Lin & London, 2013](#)). These authors also confirmed that the toxin does not bind to epicholesterol, a raft-promoting  $3\alpha$ -OH sterol. Using a Förster resonance energy transfer assay in model membrane vesicles containing coexisting ordered and disordered lipid domains, perfringolysin O preferentially partitioned into ordered domains in vesicles containing high and low-transition temperature lipids plus cholesterol or 1:1 (mol/mol) cholesterol/epicholesterol, whereas they preferred disordered domains in vesicles containing high-T<sub>m</sub> and low-T<sub>m</sub> lipids plus 1:1 (mol/mol) coprostanol/epicholesterol. The authors concluded that the association of proteins with ordered lipid domains is dependent upon both the association of the protein-bound sterol with ordered domains and hydrophobic match between the transmembrane segments and the ordered domains ([Lin & London, 2013](#)). One of the first cytochemical applications of perfringolysin using fluorescence microscopy revealed the sequestration of cholesterol in caveolae ([Fujimoto, Hayashi, Iwamoto, & Ohno-Iwashita, 1997](#)). The proteolytically-modified and biotinylated perfringolysin O has been used to image cholesterol-rich membranes by electron microscopy ([Möbius et al., 2002](#)).

An important biotechnological step towards the obtention of perfringolysin O in pure form and sufficient amounts was the cloning and expression of the gene coding for this cytolysin ([Tweten, 1988](#)). This enabled the characterization of peptide cleavage products of the toxin, such as the enzymatically cleaved C-terminal domain 4 (D4 fragment) that interacts with sterols ([Nelson, Johnson, & London, 2008](#)) and derivatization with fluorophores. The toxin's capacity to recognize cholesterol above a certain concentration in the exofacial leaflet of the plasma membrane has been exploited to produce various cholesterol biosensors, mostly based on fluorescent derivatives of the protein or its peptide fragments. A biosensor based on the D4 from *Clostridium perfringens* perfringolysin O toxin was found to recognize cholesterol in the inner leaflet of the plasma membrane ([Maekawa & Fair, 2015](#)).

The genetically-encoded cholesterol biosensor based on the fourth domain of *C. perfringens* theta-toxin, D4H, was shown to recognize cholesterol in the cytoplasmic-facing leaflet of the plasma membrane and organelles ([Maekawa & Fair, 2015](#)). D4H disassociates from the plasma membrane upon cholesterol extraction and after perturbations of cellular cholesterol trafficking. When used in combination with a recombinant version of the biosensor, these authors found that phosphatidylserine was essential for retaining cholesterol in the cytosolic leaflet of the plasma membrane. The authors indicated that the sensor is suitable for super-resolution microscopy applications.

The D4 peptide coupled to the green fluorescent protein (D4-GFP) and the biotinylated derivative (BCtheta) were reported to label specifically cholesterol-rich lipid domains (Ohno-Iwashita et al., 2004; Waheed et al., 2001) following biochemical criteria (detergent extraction with sucrose gradient centrifugation and enrichment in detergent-resistant membranes). The probes were also employed to determine whether the inner leaflet of the plasma membrane contained cholesterol-rich domains isolated using biochemical procedures. According to this criterion, the cytoplasmic-facing hemilayer was found to contain cholesterol-enriched domains (Hayashi, Shimada, Inomata, & Ohno-Iwashita, 2006). D4-GFP was also used to measure cholesterol content in the plasma membrane by flow cytometry (Wilhelm, Voilquin, Kobayashi, Tomasetto, & Alpy, 2019). Another fluorescent adduct (with enhanced GFP), EGFP-D4, was used to validate the inner-leaflet preferential partition of cholesterol in the bilayer. Controlled expression levels of wild-type EGFP-D4 and several mutants thereof showed that wild-type EGFP-D4 did not localize in the plasmalemma, whereas the D434A mutant did (Buwaneka, Ralko, Liu, & Cho, 2021). The specificity of perfringolysin O and its derivatives for cholesterol-rich Lo lipid domains contrasts with that of filipin, which binds in a non-specific manner to cholesterol.

Cholesterol is known to activate mTORC1 kinase, considered to be the master growth regulator, by recruiting the enzyme to the lysosomal surface. This activation requires the delivery of cholesterol across endoplasmic reticulum-lysosomal contacts via cholesterol carrier proteins like the oxysterol binding protein (OSBP). In cells lacking OSBP, the recruitment of mTORC1 is inhibited due to impaired cholesterol transport to lysosomes (Lim et al., 2019). These authors used the red fluorescent probe mCherry to label D4H\*, an improved version of the original D4H in which Y415A and A463W mutations were introduced, and which binds to membranes when cholesterol exceeds 10% molar content. In non-permeabilized cells, the new biosensor mCherry-D4H\* labeled only the outer leaflet of the plasmalemma. The probe was delivered to the cell interior via a liquid nitrogen pulse that permeabilized the plasma membrane but left intact the lysosomal membrane. mCherry-D4H\* did not bind to lysosomal membranes, indicating cholesterol content below 10%. In contrast, the sensor bound to lysosomal membrane from patients carrying the pathogenic NPC1 mutant characteristic of Niemann-Pick disease type C (Lim et al., 2019).

### 3.4 Fluorescent theonellamides

Theonellamides are bicyclic dodecapeptides from marine sponges of the genus *Theonella*. They have cytotoxic and antifungal properties, inhibiting yeast cell growth by interfering with the endogenous sterol, ergosterol. Fluorescently-labeled derivatives of theonellamides (e.g. aminomethyl-coumarin or BODIPY-FL-labelled theonellamides) have been used as sterol sensors, recognizing 3 $\beta$ -hydroxy-sterols like cholesterol and ergosterol. In mammalian cultured cells the probes display a patchy distribution in the plasma membrane, similar to that exhibited by filipin. Although theonellamides exhibit low membrane permeability, they also label intracellular organelles (Nishimura et al., 2013).

### 3.5 Sterol-transfer protein, Osh4

The oxysterol-binding protein-related proteins (Orp) are conserved from yeast to humans and are implicated in the regulation of sterol homeostasis and in signal transduction pathways. Osh/Orp proteins transport sterols between organelles and are involved in phosphoinositide metabolism. Osh4 is one such yeast cytosolic sterol transfer protein known to bind cholesterol and 25-hydroxy-cholesterol and transport these sterols to the ER; in exchange it transports phosphatidylinositol-4-phosphate (PI(4)P) back (de Saint-Jean et al., 2011; Im, Raychaudhuri, Prinz, & Hurley, 2005). Osh4p has been shown to extract and transport dehydroergosterol, two processes inhibited by (PI(4)P) (de Saint-Jean et al., 2011). Recently eOsh4 was engineered from Osh4 to remove the sterol transfer activity and the affinity for 25-hydroxy-cholesterol and PI(4)P. eOsh4 acts as a ratiometric sensor WCR-eOsh4, which tightly binds vesicles containing low concentrations of cholesterol ( $\leq 5$  mol%). WCR-eOsh4 has high affinity and specificity for cholesterol-containing membranes and can be used to detect low-abundance cholesterol in the membrane, independent of its lipid environment (Buwaneka et al., 2021)

### 3.6 Correlative studies using fluorescent cholesterol sensors and other physical techniques

Cyclodextrins have been widely employed to manipulate the cholesterol content of biological membranes. In addition, cyclodextrins have been used to compare their ability to extract different fluorescent cholesterol analogues. Differences were observed in the kinetics of cyclodextrin-mediated extraction of NBD-cholesterol and two BODIPY-labeled cholesterol analogues from the membrane, which were followed by measuring the Förster resonance energy transfer between a rhodamine-labeled phosphatidylethanolamine and the cholesterol analogues (Milles et al., 2013). A multiplicity of factors determines the differential ability of cyclodextrin extraction, including the probes'

hydrophobicities and their orientation within the bilayer, affinity with cyclodextrin and the impact of the latter on lipid order, among other variables.

Ganglioside and SM probes tagged with BODIPY, as well as NBD cholesterol derivatives PC and SM, were imaged using fluorescence microscopy and atomic force microscopy (AFM) to test the ability of the probes to sense lipid domains (Shaw et al., 2006). The authors observed that some of the probes purported to be reporters of liquid-ordered (raft) lipid domains partitioned into non-raft regions of the membrane, warranting caution in the use of fluorescence microscopy as the sole criterion for lipid domain identification.

Photolabeling techniques can afford a high degree of specificity to identify the amino acid residues in the target protein. A powerful combination is obtained by adding a fluorescent tag to the photolabeling compound. This has recently been accomplished with a series of cholesterol analogue photolabeling reagents to which fluorescent tags (e.g. the red-emitting TAMRAzide (5-carboxytetramethylrhodamine-azide)) were attached via click chemistry on their alkyne moiety. These cholesterol-mimetic compounds retain cholesterol's ability to suppress HMG-CoA synthase, the key enzyme for the de novo cholesterol synthesis, and may prove useful not only for identifying cholesterol sites on transport proteins but also for identifying the subcellular localization of the incumbent carrier proteins in dynamic studies of cholesterol trafficking.

### 3.7 Probes for specific phospholipids

Recent years have witnessed the design and production of sensors exploiting the known affinity of proteins for certain lipids and enzymes involved in lipid metabolism. These developments were aided by the discovery of fluorescent proteins and the biotechnology of these proteins. Fluorescent proteins currently cover a wide palette of the visible spectrum and new variants are increasingly being produced in the far-red/near-infrared and infrared regions, partly in response to requirements in the field of super-resolution microscopy. In this section, the use of fluorescent proteins is exemplified in their application to the study of some phospholipid membrane classes.

### 3.8 Polyphosphoinositide

Despite their relatively low amounts in membranes, polyphosphoinositides (poly-PIs) are an important class of lipids involved in the vesicular transport of proteins and lipids between the different compartments of eukaryotic cells, budding, membrane fusion, and cytoskeleton dynamics. Dysregulation of the enzymes involved in their metabolism is increasingly being related to oncogenesis, myopathies, and neuropathies (see review in (De Craene, Bertazzi, Bär, & Friant, 2017)). Tamas Balla and coworkers have for years studied the cell biology of this key class of lipids and the involvement of pleckstrin homology (PH) domains. Early studies characterized the role phospholipase C  $\delta$ , which specifically binds PtdIns(4,5)P<sub>2</sub>. One of the probes developed towards this end was the green fluorescent protein variant GFP-PH-PLC, the GFP-tagged PH domain of the phospholipase C  $\delta$  (Varnai & Balla, 1998).

Other poly-PI sensors were subsequently developed, like the one employing the PtdIns4P binding domain of SidM (P4M) of the secreted effector protein SidM from the bacterial pathogen *Legionella pneumophila*. A green fluorescent protein adduct, GFP-P4Mx2 (GFP-conjugated tandem fusion of P4M domain consisting of amino acids 546–647 of *Legionella pneumophila* SidM) was produced to investigate the distribution of phosphatidylinositol 4-phosphate (PtdIns4P). Pools of this poly-PI were found in Golgi membranes, the plasma membrane, and Rab7-positive late endosomes/lysosomes (Hammond, Machner, & Balla, 2014), reflecting the wide distribution of this lipid class in the cell.

### 3.9 Phosphatidylserine

Using quick-freeze and freeze-fracture replica labeling electron microscopy it was recently possible to establish the transbilayer distribution of PS in the ER membrane (Tsuji et al., 2019). PS was found to reside predominantly in the exofacial, cytoplasmic-facing leaflet of the membrane. PS is maintained in the cytosolic face of the ER membrane by a mechanism similar to that operating in the plasmalemma that depends on TMEM16K family scramblases (Tsuji et al., 2019). The probe used by Tsuji and coworkers to identify PS was based on the protein evectin-2 (GST-2xPH) and its mutant GST-2xPH(K20E). Evectin-2 is a recycling endosome-resident protein (Kay & Fairn, 2019) essential for the retrograde transport from recycling endosomes to the trans-Golgi network (Uchida et al., 2011). Evectin-2 contains an N-terminal pleckstrin homology (PH) domain and a C-terminal hydrophobic region. It is the PH domain of evectin-2 that binds PS specifically. Green fluorescent protein (GFP) derivatives of two evectin-2 molecules in tandem (GFP-

Evt2PH) (Uchida et al., 2011) were recently used by Li and coworkers (Li et al., 2021) as a live-cell sensor of PS together with Lact-C2-GFP, another genetically encoded fluorescent PS biosensor based on the C2 domain of lactadherin (Lact-C2) (Yeung et al., 2008). Li and collaborators contrast live-cell sensors (GFP-Evt-2PH and Lact-C2-GFP) with “purified” sensors like GST-2xPH, the evectin fluorescent protein used by Tsuji and coworkers in their electron microscopy work (Tsuji et al., 2019).

The members of the evolutionarily conserved GRAMD1 family of ER-resident transport proteins (GRAMD1a/1b/1c) are known for their involvement in cholesterol homeostasis through regulated transport of the “accessible” cholesterol pool from the plasma membrane to the ER (see review in (Naito & Saheki, 1866)). The participation of the GRAMD1 proteins in lipid homeostasis goes beyond this important function: they harbor separate but structurally neighboring sites for cholesterol and anionic lipids like PS in their GRAM domain. This allows GRAMD1 proteins to function as a coincidence detector for cholesterol and PS (Ercan, Naito, Koh, Dharmawan, & Saheki, 2021). Some domains, including PH domains, contain synergistic binding sites that each exhibit low affinity for the two lipids. The simultaneous binding of two lipids to an individual domain occurs synergistically when both lipids are present in the target membrane (Lemmon, 2008). Ercan and coworkers stably expressed a fluorescence derivative of GRAMD1b (GFP-GRAM1b WT) and its mutant G187L (GFP-conjugated GRAM domain of GRAMD1b with a single G187L mutation in TKO cells) to follow the recruitment of the GRAMD1b protein to the ER and plasma membrane and the influence of the G187L mutation on GRAMD1-dependent cholesterol transport.

### 3.10 Phosphatidic acid

Structurally, phosphatidic acid (PA) is the simplest glycerophospholipid and a minority component in membranes. Despite its low abundance, it is a structural determinant of membrane shape depending on its location in the bilayer and displays various other roles, including second messenger functions in important cellular mechanisms, vesicular trafficking, cytoskeletal organization, secretion and cell proliferation (Liu, Su, & Wang, 2013). Proteins that possess PA binding domains like the yeast proteins Spo20p, Opi1p and Raf1 constitute possible targets for fluorescence derivatization. Spo20p has been found in the plasma membrane of mammalian cells and Opi1 p shuttles between ER and nuclear membranes. Fragments of these proteins containing the PA-binding domain were obtained as fusion proteins in *E. coli* by Vitale and coworkers (Kassas et al., 2017). Phagocytic cells like the macrophages require phospholipase-generated PA to remodel their plasma membrane and augment their surface area during phagocytosis. The GFP-fused PA-binding protein probes and GFP-PDE4A1, a GFP-tagged single exon in the unique N-terminal region of the cAMP-specific phosphodiesterase, were used to study the affinity of the binding domain for PA, the intracellular sites of PA synthesis in the course of phagocytosis, and the recruitment of PA to the plasma membrane (Kassas et al., 2017).

### 3.11 Glycerol-3-phosphate acyltransferase

SEIPIN is a protein implicated in both adipogenesis and lipid droplet expansion that interacts with microsomal isoforms of glycerol-3-phosphate acyltransferase (GPAT). Abnormally elevated in SEIPIN-deficient cells, this enzyme is associated with the block in adipogenesis and abnormal lipid droplet morphology observed in loss-of-function mutations in SEIPIN related with the Berardinelli-Seip congenital lipodystrophy 2 syndrome (Pagac et al., 2016). These authors designed a series of sensors (mCherry-tagged GPAT4, HA-tagged seipin, GFP-tagged seipin, mCherry-tagged seipin, and a combined HA/GFP/mCherry-fused human seipin) to study the relationship between the enzyme, SEIPIN, and the lipodystrophy.

## 4 Sensing membrane polarity

The issue of membrane polarity -often termed “membrane fluidity”- has been approached by a variety of biophysical methods such as electron spin resonance, nuclear magnetic resonance, and fluorescence spectroscopy. The three methodologies require appropriate sensors. In the fluorescence spectroscopy approach, fluidity of biomembranes is sensed indirectly through measurement of the polarity of the probe’s microenvironment, usually reflected in characteristic spectral signatures of the probe calibrated in membrane-mimetic systems (Klymchenko, 2017).

### 4.1 Laurdan

Laurdan (6-dodecanoyl-2-dimethylamino naphthalene) was conceived by Gregorio Weber, together with other similar fluorescent probes like Prodan (6-propionyl-2-dimethylaminonaphthalene) as an environmental sensor (Weber & Farris, 1979). Laurdan was initially applied to characterize the polarity of protein regions in bovine serum albumin and myoglobin, and introduced in membrane biophysics only years later (Parasassi, Conti, & Gratton, 1986). The groups of Parasassi, Gratton, Bagatolli and Gauss have contributed a variety of methodological developments covering both static and dynamic imaging modalities that contributed to establishing Laurdan not only as the gold standard in solvatochromic membrane polarity sensing but also as a reference multi-sensor of membrane-related phenomena (Bagatolli, Gratton, & Fidelio, 1998; Bagatolli, Maggio, Aguilar, Sotomayor, & Fidelio, 1997; Fiorini, Curatola, Kantar, Giorgi, & Gratton, 1993; Gaus et al., 2003; Gaus, Zech, & Harder, 2006; Levi, Wilson, Cooper, & Gratton, 1993; Parasassi, De Stasio, d'Ubaldo, & Gratton, 1990; Parasassi, De Stasio, Ravagnan, Rusch, & Gratton, 1991; Parasassi, Di Stefano, Ravagnan, Saporita, & Gratton, 1992; Parasassi & Gratton, 1992; Parasassi, Loiero, Raimondi, Ravagnan, & Gratton, 1993a, 1993b; Parasassi, Ravagnan, Rusch, & Gratton, 1993). Since it first began to be used forty years ago, Laurdan has become a well-established tool and continues to provide information in both cuvette fluorimetry and fluorescence microscopy studies.

Laurdan exhibits high sensitivity to the polarity of its environment and to the molecular dynamics of the surrounding dipoles. Dipolar relaxation processes are reflected as relatively large spectral shifts of its emission (Weber & Farris, 1979). Measurements of the so-called general polarization (GP) of Laurdan exploit its advantageous spectral properties, as initially measured by time-resolved fluorescence emission spectra in cuvette studies (Parasassi et al., 1986). Laurdan's molecular structure dictates the positioning of its lauric acid acyl chain in the bilayer hydrophobic core and its naphthalene aromatic ring at the hydrophilic/hydrophobic interface region of the membrane bilayer. In this region, the overwhelming "solvent" surrounding Laurdan naphthalene moiety is made up of dipole-carrying water molecules. Laurdan senses the relaxation rates of these water dipoles, with rotational times in the range of its fluorescence lifetime (Parasassi, Krasnowska, Bagatolli, & Gratton, 1998) and hence it reports on the vicinal dielectric milieu: when no relaxation occurs Laurdan fluorescence emission is blue-shifted and GP values are high, indicating low water content (and mobility), coincident with a tight packing of the lipid acyl chains such as observed in the liquid-ordered lipid phase. Laurdan does not show preference for a single lipid phase, partitioning ubiquitously into both Ld and Lo phases. The liquid-disordered phase allows more water molecules to populate the interface region; Laurdan senses the dipolar relaxation of this larger number of water molecules, affecting its own excited state dipole moment (Weber & Farris, 1979) and resulting in red-shifted emission and lower GP values. The position of the fluorescence emission maxima (~ 440 nm in the gel phase and 490 nm in the liquid-disordered phase) is maintained over a wide range of temperatures (Antollini et al., 1996; Bacalum, Zorilă, & Radu, 2013).

These properties of Laurdan fluorescence can be translated into the fluorescence microscopy realm to provide topographical information. Early measurements undertaken in membrane-mimetic synthetic lipid systems and isolated native membranes using two-photon microscopy led to the visualization of lateral heterogeneities in membranes rendered by Laurdan GP (Parasassi, Gratton, Yu, Wilson, & Levi, 1997). This paved the way for characterization of the domain separation and coexistence in GUVs (Bagatolli & Gratton, 1999; Bagatolli, Parasassi, & Gratton, 2000; Montes, Alonso, Goni, & Bagatolli, 2007) and planar bilayers (Brewer, de la Serna, Wagner, & Bagatolli, 2010). Laurdan GP in combination with fluorescence correlation spectroscopy (FCS) was subsequently employed to probe cell membrane heterogeneity and detect nanoscopic mobile structures, presumably lipid domains, containing tightly packed molecules (Sanchez, Tricerri, & Gratton, 2012).


Application of the phasor geometric plot method (Jameson, Gratton, & Hall, 1984) to fluorescence lifetime imaging (FLIM) of Laurdan in the fluorescence microscope opened up new possibilities to visualize membrane heterogeneities - lipid domains - with enhanced precision. Recent reviews discuss the contributions of the phasor approach and its applications to hyperspectral analysis and lifetime imaging (Gunther, Malacrida, Jameson, Gratton, & Sánchez, 2021; Ranjit, Malacrida, Jameson, & Gratton, 2018). The FLIM-phasor combination using Laurdan fluorescence lifetime was first applied to study the influence of cholesterol content and changes in membrane fluidity and phospholipid order in live cell measurements ((Golfetto, Hinde, & Gratton, 2013); reviewed in (Golfetto, Hinde, & Gratton, 2015)). Dual-channel recording of Laurdan FLIM with the phasor method facilitates the dissection (unmixing) of up to three components of the image (Fereidouni, Bader, & Gerritsen, 2012). In the case of Laurdan, the interesting distinction is between environmental polarity information vs. dipolar relaxation phenomena informing on water content in the membrane.

We have used Laurdan to explore the lipid microenvironment of the paradigm fast ligand-gated ion channel, the neurotransmitter receptor for acetylcholine. To this end we introduced a hitherto unexploited property of the probe, i.e. its ability to act as a Förster resonance energy transfer (FRET) acceptor of tryptophan emission, using the transmembrane tryptophan residues of the nicotinic receptor as donors. We were thus able to characterize the physical state of environmental lipids within Förster distances from these membrane-embedded tryptophan residues in a native membrane environment (Antollini et al., 1996; Antollini & Barrantes, 1998; Antollini & Barrantes, 2002) (reviewed in **Q5** (Antollini & Barrantes, 2007)) and see Chapter 7 in this volume on the evaluation of membrane structure by Laurdan imaging.

#### 4.2 di-n-ANEPPDHQ

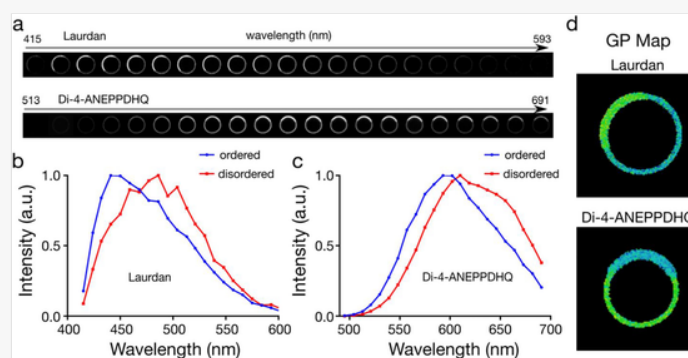
In the early 90s Loew and coworkers introduced di-4-ANEPPS, the naphthyl analogue of the aminostyryl class of fluorescent dyes, as a fast potentiometric sensor for membrane studies (Loew et al., 1992). The compound exhibits an increase in fluorescence emission together with a red shift of its excitation spectrum upon hyperpolarization of the membrane. Di-4-ANEPPDHQ is one in a series of naphthylstyryl-pyridinium (di-n-ANEPPDHQ) fluorescent compounds introduced subsequently by Loew and his group (Obaid, Loew, Wuskell, & Salzberg, 2004). These probes have the same chromophore as the potentiometric sensor di-8-ANEPPS and the quaternary ammonium headgroup (DHQ) of RH795, thus resulting in two positive charges vs the neutral propylsulfonate-ring nitrogen combination (Obaid et al., 2004). Di-4-ANEPPDHQ can discriminate between liquid-ordered phases and liquid-disordered phases coexisting in model membranes using either linear or nonlinear microscopies (Jin, Millard, Wuskell, Clark, & Loew, 2005). The fluorescence emission spectrum of di-4-ANEPPDHQ is blue-shifted  $\sim 60$  nm in the liquid-ordered phase (emission maximum 610 nm) compared with the liquid-disordered phase (emission maximum 560 nm) and exhibits strong second harmonic generation in the liquid-disordered phase compared with the liquid-ordered phase. These spectral changes can be conveniently followed by the simple GP approach based on the linear combination of the emission maxima. Tested in large unilamellar lipid vesicles, di-4-ANEPPDHQ showed a cumulative 60-nm difference in emission spectra in cholesterol-containing LUVs in the liquid-ordered state versus cholesterol-free vesicles in the liquid-disordered phase (Jin et al., 2006).

Using GP measurements, a comparative study of Laurdan vs di-4-ANEPPDHQ found the former to be more sensitive to temperature, and the naphthylstyryl probe more sensitive to cholesterol content (Amaro, Reina, Hof, Eggeling, & Sezgin, 2017). As shown in Fig. 4, the two probes exhibit an environmentally-sensitive shift in their emission spectra and can be used in a complementary manner to image simultaneously coexisting phases in the same specimen.

 Images are optimised for fast web viewing. Click on the image to view the original version.

alt-text: Fig. 4

Fig. 4





Generalized polarization (GP) imaging of Laurdan and di-4-ANEPPDHQ in giant plasma membrane-derived vesicles with coexisting phases. (A) Spectral images of the vesicles. (B, C) fluorescence emission spectra of Laurdan and di-4-ANEPPDHQ in liquid-ordered (red) and disordered (blue) lipid domains coexisting in the vesicles. (D) Fluorescence microscopy images mapping the coexisting distribution of the two probes on the perimeter of the giant vesicles.

Reproduced from Amaro, M., Reina, F., Hof, M., Eggeling, C., & Sezgin, E. (2017). Laurdan and Di-4-ANEPPDHQ probe different properties of the membrane. *Journal of Physics D: Applied Physics*, 50(13), 134004. doi:10.1088/1361-6463/aa5dbc under the terms of the Creative Commons Attribution 3.0 license.

We have employed di-4-ANEPPDHQ imaging in an attempt to observe the distribution of ordered and disordered lipid regions and their topographical relationship to the location of the nicotinic acetylcholine receptor at the plasma membrane (Kamerbeek et al., 2013). We found that the receptor protein, imaged with fluorescent antibodies, was roughly equally distributed between diffraction-limited liquid-ordered and disordered domains. The proportion of receptor aggregates associated with liquid-ordered domains diminished upon cholesterol depletion, and this was accompanied by a decrease in di-4-ANEPPDHQ GP values.

## 5 Super-resolution microscopy triggers the development of new sensors

Super-resolution optical microscopy (nanoscopy) revolutionized and revived light microscopy, establishing new standards in fluorescence microscopy (Hell, 2015). It has currently acquired the status of a mature technique and the applications cover a wide spectrum in many disciplines of biology, physics, materials science, microbiology, biotechnology, and chemistry (Betzig, 2015; Moerner, 2015).

The revolutionary facet of nanoscopy is related to its ability to circumvent the century-old dogma, the diffraction-barrier of light (Abbe, 1873): the degree of detail that can be resolved by a conventional light microscope is fundamentally limited by diffraction. Imaged with conventional lenses, an infinitely small point source produces a spot of finite volume, the point spread function (PSF), and two such small point sources that are closer together than the half-width of the PSF half-width will overlap and be observed as a single object. The resolution in the focal plane can be approximated as  $0.5 \lambda / \text{N.A.}$ , with  $\lambda$  being the wavelength of light and N.A. the numerical aperture of the objective lens. Using visible light ( $\lambda \sim 550$  nm) and a high-N.A. objective lens (N.A.  $\sim 1.4$ ) the attainable resolution is  $\sim 200$  nm. Nanoscopy has gone beyond this diffraction barrier, and this achievement was accompanied by corresponding advances in the design and chemical synthesis of organic compounds that fulfill the requirements of a given super-resolution microscopy modality.

Resolution can be improved by restriction of the fluorescence emission to an area much smaller than the PSF. Stimulated emission depletion (STED) nanoscopy is a direct scanning modality of super-resolution optical microscopy whose essential principle is the de-activation of fluorophores in the immediate perimetric volume surrounding the interrogating beam, thereby spatially confining the emission volume (Hell & Wichmann, 1994).

Under conditions used for single-molecule detection, photobleaching follows a two-step mechanism (Eggeling, Widengren, Rigler, & Seidel, 1998). The collision of  $^3\text{O}_2$  molecular oxygen with the long-lived triplet state of fluorophores depletes the latter via triplet-triplet energy transfer annihilation, quenching fluorescence emission and returning the fluorophore to its ground singlet-state. In addition, reactive oxygen species such as singlet oxygen ( $^1\text{O}_2$ ), superoxide, and hydroxy radical are produced (Helmerich, Beliu, Matikonda, Schnermann, & Sauer, 2021). The reactive oxygen species is doubly damaging in fluorescence microscopy since it hampers cell viability, reduces the fluorescence count rate in STED and induces blinking of single-molecule localizations in the other family of super-resolution microscopy modalities, the single-molecule localization microscopies (SMLM). In the latter approach, fluorophores are stochastically switched on ("blink") and off ("blink"), and the localizations are estimated off-line by computing the centroids of their point-spread functions. The accuracy of the localizations depends on the density of the fluorophores and the number of photons collected per localization. Nanoscopy has therefore required special attention to the buffer conditions for fixed and live-cell imaging containing antioxidants such as *n*-propyl gallate, *p*-phenylenediamine or ascorbic acid to mitigate the effects of reactive oxygen species (Henriques, Griffiths, Hesper Rego, & Mhlanga, 2011) and optimization of fluorescent probes for STED (Connor, Byrne, Berselli, Long, & Keyes, 2019; Man et al., 2021; Nizamov et al., 2016; Xu et al., 2020) and of switchable probes for live-cell and SMLM (Grimm et al., 2015; Grimm et al., 2016; van de Linde, Heilemann, & Sauer, 2012) imaging modalities.

In the STED modality of nanoscopy, the off-switching of the fluorescence emitters by the doughnut-shaped depletion volume allows only the central emitters in the "on" emission state to contribute their photons during scanning (

Wildanger, Rittweger, Kastrup, & Hell, 2008). The resolution increases as the depletion beam increases and restricts emission to smaller volumes. The number of possible excitation cycles that the fluorescent probe can withstand is an important requisite for the success of the STED technique, and this depends on the photophysical stability of the fluorophore (Gould, Hess, & Bewersdorf, 2012; van der Velde, Smit, Punter, & Cordes, 2018).

Photobleaching, the irreversible diminution of the fluorescence emission, or its transient counterpart, the conversion of the fluorophore into non-emissive species (“blinking”) (Ha & Tinnefeld, 2012) can occur via intersystem crossing, chemical reactions, or redox processes that are enhanced in the case of fluorophores lying inside the cell, where the presence of e.g. glutathione or nicotinamide adenine dinucleotide compromise fluorescence emission intensity. The high (de)excitation illumination conditions imposed by nanoscopy have posed special requirements in terms of photostability of the probes. A major effort has been devoted to the design of new strategies for the organic synthesis of suitably photostable and photoconversion-resistant fluorophores, or probes for spectral unmixing, spectrally-resolved lifetime imaging and other nanoscopic modalities. Rhodamines (Bossi, Belov, Polyakova, & Hell, 2006; Boyarskiy et al., 2008), caged NN rhodamines (Belov, Wurm, Boyarskiy, Jakobs, & Hell, 2010) and cell-penetrant rhodamine and fluorogenic carbopyronines with absorption maxima in the 500–630 nm region have been synthesized for live-cell STED microscopy (Butkevich et al., 2016). These probes are amenable to emission depletion via orange-red (618 nm) and near-infrared (775 nm) lasers. Triarylmethane fluorophores with increased stability and in particular improved resistance to oxidative “photoblinking” via photoconversion, also aimed at STED microscopy of living cells (Butkevich, Bossi, Lukinavičius, & Hell, 2019) have been recently incorporated into this repertoire of new fluorescent probes.

Blue-shifted fluorescence excitation and emission maxima (hypochromic shift) in the range of 660-735 nm have been reported to occur with the photoproducts of far-red absorbing cyanine dyes Cy5 and Alexa-Fluor647. With the latter probe, anomalous emission due to a photoconverted blue-shifted fluorescent product of the cyanine core was observed when imaging HIV virions at the cell surface, and attributed to the high irradiation at 561 nm or 488 nm in addition to the 644 nm absorption maximum of the fluorophore (Dirix et al., 2018). The opposite, bathochromic shift (“photoredding”) has also been reported for some fluorophores. Fluorophore photobleaching and blinking are both accompanied by diminution of the fluorescence intensity, whereas photoblinking of photoredding lead to spectral inconsistency and misidentification of spectral signals, particularly important in multicolor fluorescence microscopy.

The now well-established HaloTag method is used in most cases to incorporate the fusion proteins into living cells. The HaloTag technique relies on the use of a protein sensor genetically fused to an engineered enzyme (modified *Rhodococcus rhodochrous* dehalogenase), which covalently links the protein of interest to its target. Only the 6'-carboxy isomers of the above rhodamine and fluorogenic carbopyronines have been successfully employed to tag proteins.

Photoactivatable fluorescent probes have so far had little application in STED microscopy due to their low solubility in aqueous media and because they require two-photon activation via the STED beam. Hell and coworkers have recently reported the synthesis of ONB-2SiR, a fluorophore that can be both photoactivated in the UV region and specifically de-excited by STED at 775 nm (Weber et al., 2021).

One field of fluorescence microscopy that has benefited enormously from the combined efforts of biology and organic chemistry is that of fluorescent proteins. Developments in this area have provided cell biologists the opportunity to exploit various photophysical properties of fluorescent proteins, i.e. photo-transformations like photo-switching (as used in STORM nanoscopy (Bates, Huang, Dempsey, & Zhuang, 2007; Bates, Huang, & Zhuang, 2008)), photoactivation (as exploited in PALM (Hess, Girirajan, & Mason, 2006; Manley et al., 2008)) or photoconversion (as utilized in PALM microscopy with mEos or Dendra2 fluorescent proteins (Adam et al., 2011)). The reader is referred to several reviews on the applications of fluorescent proteins (Fernández-Luna, Coto, & Costa, 2018; Kremers, Gilbert, Cranfill, Davidson, & Piston, 2011; Truong & Ferré-D'Amaré, 2019). Fluorescent proteins have been successfully used to trace proteins in cells, study the localization of membrane proteins or follow their lateral motion in living cells (Manley et al., 2008), but they have still not been applied in lipid domain studies. Due to their much lower background and phototoxicity compared to proteins with fluorescence emission in the visible region of the spectrum (Tosheva, Yuan, Matos Pereira, Culley, & Henriques, 2020), infrared fluorescent proteins offer interesting possibilities for development and application in super-resolution microscopy. This is a needy area and an opportunity for the bioengineering field, given the scarcity of near-infrared and infrared-emitting proteins with great potential for live-cell nanoscopy imaging (Hense et al., 2015; Matlashov et al., 2020; Shcherbakova et al., 2016; Yu et al., 2014).

The availability of new organic fluorophores suitable for super-resolution imaging has impacted on the field of lipid membrane domains, given the nanometric dimensions of these lateral heterogeneities and the increased resolution afforded by nanoscopy. GUVs and their analogous giant plasma membrane vesicles obtained from cells are convenient objects to test fluorescent sensor molecules in parallel under identical experimental conditions. That is precisely the strategy followed by Petra Schwille and coworkers in order to compare the behavior of several fluorescent lipid domain sensors. Label size, polarity, charge, and position of the probes on the one hand, and lipid headgroup and membrane composition on the other determined the complex partitioning of the sensors (Sezgin et al., 2012). “Raft” lipid analogues partitioned preferentially into the giant plasma membrane vesicles, whereas in synthetic GUVs they partitioned into liquid-disordered lipid domains.

A fluorescent glycerophospholipid analogue consisting of a saturated 18-carbon acyl chain PE and a hydrophilic far-red emitting fluorophore (KK114), tethered to the head group of PE by a long polyethylene glycol (PEG) linker, was synthesized to probe diffusion characteristics of lipids in membranes (Honigmann, Mueller, Hell, & Eggeling, 2013). The lateral diffusion of the probe was studied with fluorescence correlation spectroscopy in the STED mode (STED-FCS), a technique which interrogates molecular motions in the femtoliter volumes interrogated by this technique. On a mica support, the lipid analogue diffuses freely in both the Ld and Lo phases, with diffusion coefficients of  $1.8 \mu\text{m}^2 \text{s}^{-1}$  and  $0.7 \mu\text{m}^2 \text{s}^{-1}$ , respectively. Unlike most far-red emitting fluorescent lipid analogues, KK114-PEG-PE partitions predominantly into Lo domains in phase-separated ternary bilayers, but the tightly-packed lipid acyl chains in the Lo phase only slow down diffusion without producing anomalous sub-diffusion. In contrast, STED-FCS measurements on mica-supported membranes showed anomalous sub-diffusion, which the authors attributed to the transient partitioning of the lipid analogue into lipid domains of nanoscopic dimensions, where diffusion is slowed down.

A pyrene-based fluorescent ceramide conjugate, PyLa- C17Cer, has been synthesized and applied to living cells to identify lipid droplets using STED microscopy (Connor et al., 2019). The parent compound, PyLa, is a pyrene carboxyl core appended with 3,4-dimethylaminophenyl moiety. The probe permeates inside the cell and exhibits high fluorescent quantum yield, mega-Stokes shift, high photochemical stability, and low cytotoxicity. Since it does not show triplet emission at low temperatures, the authors suggest its use for fluorescence correlation spectroscopy (FCS), a highly suitable spectroscopic technique to match STED for the study of lipid dynamics in membranes (Eggeling, 2015).

The solvatochromic probe di-4-ANEPPDHQ introduced by Loew and colleagues has been employed as a sensor of membrane physical status. We employed this probe to depict the partitioning between ordered and disordered regions of the plasmalemma with diffraction-limited resolution in wide-field microscopy (Kamerbeek et al., 2013). In super-resolution microscopy, the probe has recently been used to map the lipid environment with sub-diffraction resolution on length scales below 300 nm (Nieves & Owen, 2020). A drawback of solvatochromic dyes is that they report on the membrane order of lipid domains but fail to provide accurate information about their lipid and protein composition (Lorizate et al., 2021).

The ability to measure the fluorescence spectra of individual fluorescent probes in a standard wide-field microscope added a new dimension to the fingerprinting of molecules via fluorescence microscopy. The rationale behind this approach is that averaging all photons stemming from multiple fluorescence emissions from a given fluorophore species into a single detector device sacrifices valuable information contained in the individual spectrum of each molecule. Using a grating or prism in the optical path of the microscope and an imaging detector to disperse the emission spectrum, however, diffracted images of fluorescent nanospheres with emission maxima separated by  $< 20 \text{ nm}$  and of single fluorescent probe molecules with  $30 \text{ nm}$  separation could be obtained (Heider, Barhoum, Peterson, Schaefer, & Harris, 2010). Based on this principle Xe and coworkers employed super-resolution microscopy to spectrally resolve peroxisomes, vimentin filaments, microtubules, and the outer mitochondrial membrane in fixed PtK2 cells. The method was coined spectrally-resolved STORM (Zhang, Kenny, Hauser, Li, & Xu, 2015). A gain in spatial resolution of  $\sim 10 \text{ nm}$  was already apparent when adding the spectroscopic signature of the photon-emitting molecule, i.e. a four-fold improvement over photon localization without spectral discrimination (Dong et al., 2016). The group of Samuel Hess developed similar approaches using PALM single-molecule localization microscopy. In the spectrally-resolved modality, PALM imaging of fluorescent proteins having partially overlapping emission spectra like Dendra2-hemmagglutinin, PAmCherry-cofilin or PAmKate-transferrin receptor could be resolved at the single-molecule level (Mlodzianoski, Curthoys, Gunewardene, Carter, & Hess, 2016).

Nile Red (Nile Blue A oxazone), a low molecular weight organic chemical used for decades as a dye to label intracellular lipid storages in classical histological and histopathological studies, has found new applications in super-resolution imaging using the PAINT technique to localize single-molecules and extract spectral information; the acronym sPAINT (spectral PAINT) was coined in this case (Bongiovanni et al., 2016). This superresolution modality was applied to calibrate Nile Red properties on synthetic 10 nm unilamellar vesicles of known lipid composition and to measure the hydrophobicity of the plasmalemma of HEK-293 cells depleted of or enriched in cholesterol via methyl- $\beta$ -cyclodextrin. A red-shift in the mean position and a reduction of the distribution-width of hydrophobic localizations was observed for the membranes of cholesterol-depleted cells compared with control cells (Bongiovanni et al., 2016).

A very similar study was conducted by the group of Zhang using the STORM technique and Nile Red as a sensor of membrane polarity on fixed cells. They could image distinct low-polarity regions of  $\sim 100$  nm in diameter in the plasma membrane upon addition of cholesterol or treatment with cholera toxin in fixed cells but failed to find a similar pattern in native cells (Moon et al., 2017). In agreement with the results of Bongiovanni et al. (Bongiovanni et al., 2016), Zhang and coworkers observed that cholesterol depletion with methyl- $\beta$ -cyclodextrin led to a strong red-shift of the Nile Red single-molecule spectrum at the plasmalemma but not in internal organelle membranes. Addition of cholesterol led to blue-shifted emission puncta dispersed across the membrane. These observations led the authors to infer that the low-polarity regions corresponded to ordered lipid domains observable only in cholesterol-treated cells, suggesting that such domains may not be present in native cells (Moon et al., 2017). Exactly what Nile Red senses is still a matter of debate. According to Lorizate and coworkers (Lorizate et al., 2021) Nile-Red-based sensors used in recent studies (Danylchuk, Moon, Xu, & Klymchenko, 2019; Moon et al., 2017) do not report the occurrence of lipid heterogeneity in the plasma membrane of living cells but only a higher degree of order in outward and inward protrusions of the membrane, indicating a direct association of curvature with order. To overcome these constraints, a new biorthogonal cholesterol biosensor (chol- $N_3$ ) was developed and used to characterize lipid domains in the plasma membrane of live cells interrogated with STED nanoscopy, with good resolution along the axis perpendicular to the membrane and in 3D imaging of thick samples like brain slices (Lorizate et al., 2021). The size distribution of the presumptive lipid-domain STED puncta showed peaks at  $\sim 50$  and 150 nm lateral width. Other recent studies using FCS-STED nanoscopy corroborate the usefulness of Nile Red-based sensors in studies on lipid domain packing and dynamics with long acquisition times (Carravilla et al., 2021). See Chapter 10 in this Volume for a comprehensive treatment of orthogonal lipid sensors.

## 6 Conclusions and future directions

Imaging and physical characterization of lipid domains, transbilayer and lateral (in-plane) asymmetries and other biophysical properties of cell membranes have experienced major and exciting advances in the last decades. Due to their higher photostability and brightness, fluorophore-tagged (extrinsic) lipid analogues have provided a wider range of possibilities than the intrinsically fluorescent cholesterol analogues dehydroergosterol or cholestanetriol; nevertheless, both types of probes still find specific applications in membrane research, as discussed in previous sections. The number of sensors for identifying molecular components has grown to include not only a sizeable number of lipid probes but also sensors to identify different enzymes and specific membrane proteins that indirectly report on lipid domains. This repertoire of biosensors has enabled the characterization of cell-surface binding partners, endocytic trafficking, lysosomal degradation, and disease conditions affecting such physiological phenomena. In addition, new biophysical techniques have become available, allowing the study of the physical properties underlying the structural and mechanistic bases of these phenomena.

The field of artificial intelligence (AI) and object recognition has had a major explosion in recent years, catalyzed by the inception of the convolutional, multilayer (and thus “deep”) neural network termed AlexNet by Krizhevsky and coworkers (Krizhevsky, Sutskever, & Hinton, 2012) (see review in (Brent & Boucheron, 2018)). The branch of AI known as deep learning (DL) has penetrated many spheres of science. It is currently used extensively in several subdisciplines of biology, particularly in structural biology. In cryo-electron microscopy, for instance, it has become a valuable tool to automatize the “pruning” of macromolecular structures and eliminate false positives from thousands of single-molecule identifications collected via particle-picking algorithms (Sanchez-Garcia, Segura, Maluenda, Carazo, & Sorzano, 2018). DL has also found application in identifying “good” regions in electron microscope grids (Yokoyama et al., 2020), an otherwise time-consuming and tedious step, or estimating resolution in density maps (Avramov et al., 2019).

In fluorescence microscopy, DL methods are experiencing explosive developments that address many procedural steps of the different techniques and expand the current horizon of theoretical approaches to physical modeling of cell functioning. In combination with state-of-the-art molecular biology methods like genome-wide CRISPR (clusters of interspaced short palindromic repeats) screening technology, DL has recently found application in the classification of different cell phenotypes of interest upon photoactivation and isolation via flow cytometry; the approach, coined AI-photoswitchable screening (Kanfer et al., 2021).

One of the most exciting applications of DL in fluorescence microscopy is undoubtedly the training of neural networks to *predict* structures in microscope images. In this type of application, machine learning is used to train neural networks with information gained in gray-scale label-free micrographs e.g. structures in scanning or transmission electron micrographs into virtual “stained” micrographs of the same specimens (Christiansen et al., 2018; Helgadottir et al., 2021). Upon proper training, the networks can predict a given structure and color-code it for automatic identification of new samples. Working on an unstained specimen in a conventional bright-field or phase-contrast optical microscope, the DL approach replaces both the staining and the fluorescence microscopy steps with an *in silico* neural network solution that generates virtual fluorescence-stained images.

There are still some caveats. The cell is a three-dimensional object and understanding its complex organization and functioning requires tools to interrogate these two aspects concurrently, with the requisite spatial- and time-resolution imposed by the cell’s workings. The limited contrast of the cellular structures still calls for imaging approaches that tag different components with distinct identifying sensors. This is still a major limitation of imaging techniques and fluorescence microscopy: despite the wide spectrum of sensors available, they do not suffice to differentially label and individualize the thousands of molecular species present in the cell. When we speak of multi-color detection, we are still limited to a few digits of wavelengths that we can simultaneously explore. However, this is one of the problems tackled by the super-resolution microscopy method termed DNA-PAINT (DNA-based point accumulation for imaging in nanoscale topography), a nanoscopy approach that exploits programmable transient hybridization between short oligonucleotide strands (Jungmann, 2014; Schueder et al., 2017; van Wee, Filius, & Joo, 2021). One of the inherent advantages of DNA-PAINT is its ability to employ a much wider range of multiplexing than conventional fluorescence microscopy, which relies essentially in the use of multiple probes with different spectral properties, conventionally at most 3-4 (Bates et al., 2007; Dempsey, Vaughan, Chen, Bates, & Zhuang, 2011). Recently, Jungmann, Schwille and coworkers introduced a new approach for multiplexing imaging in stochastic super-resolution, a concept that should facilitate transcriptomic, proteomic and lipidomic studies of hundreds of molecular constituents. In their proof-of-concept work, they managed 124-color imaging within minutes by engineering DNA-PAINT blinking kinetics (Wade et al., 2019).

In summary, although the panoply of optical fluorescence techniques available for imaging lipid domains in cells is still limited, and suffers from various artifacts, we should be confident **in that** the ingenuity of scientific progress, **which** will **no doubt** generate new approaches, instrumentation, and techniques to tackle the simultaneous interrogation of several biophysical properties of lipid domains with enhanced temporal and spatial resolution.

## Acknowledgments

This work was written within the framework of the grant PICT 2015-2654 from the Ministry of Science, Technology and Innovative Production of Argentina.


## Author contributions

I conceived and designed the study, searched the literature, interpreted the data and wrote the manuscript. I conceived the illustrations and had technical help to produce them.

## Declaration of interests

The author declares no competing interests.

## References

 The corrections made in this section will be reviewed and approved by a journal production editor. The newly added/removed references and its citations will be reordered and rearranged by the production team.

Abbe, E. (1873). Beitrage zur Theorie des Mikroskops und der mikroskopischen Wahrnehmung. *Archiv für Mikroskopische Anatomie*, 9, 413–418. Retrieved from <https://doi.org/10.1007/BF02956173>.

Adam, V., Moeyaert, B., David, C.C., Mizuno, H., Lelimosin, M., & Dedecker, P., et al. (2011). Rational design of photoconvertible and biphotochromic fluorescent proteins for advanced microscopy applications. *Chemistry & Biology*, 18(10), 1241–1251. doi:10.1016/j.chembiol.2011.08.007.

Ahmed, S.N., Brown, D.A., & London, E. (1997). On the origin of sphingolipid/cholesterol-rich detergent-insoluble cell membranes: Physiological concentrations of cholesterol and sphingolipid induce formation of a detergent-insoluble, liquid-orderer lipid phase in model membranes. *The Biochemist*, 36(36), 10944–10953.

Amaro, M., Filipe, H.A., Prates Ramalho, J.P., Hof, M., & Loura, L.M. (2016). Fluorescence of nitrobenzoxadiazole (NBD)-labeled lipids in model membranes is connected not to lipid mobility but to probe location. *Physical Chemistry Chemical Physics*, 18(10), 7042–7054. doi:10.1039/c5cp05238f.

Amaro, M., Reina, F., Hof, M., Eggeling, C., & Sezgin, E. (2017). Laurdan and Di-4-ANEPPDHQ probe different properties of the membrane. *Journal of Physics D: Applied Physics*, 50(13), 134004. doi:10.1088/1361-6463/aa5dbc.

Antollini, S.S., & Barrantes, F.J. (1998). Disclosure of discrete sites for phospholipid and sterols at the protein-lipid interface in native acetylcholine receptor-rich membrane. *Biochemistry*, 37(47), 16653–16662. doi:10.1021/bi9808215.

Antollini, S.S., & Barrantes, F.J. (2002). Unique effects of different fatty acid species on the physical properties of the torpedo acetylcholine receptor membrane. *Journal of Biological Chemistry*, 277(2), 1249–1254. Retrieved from <http://www.ncbi.nlm.nih.gov/pubmed/11682474>.

Antollini, S.S., & Barrantes, F.J. (2007). Laurdan studies of membrane lipid-nicotinic acetylcholine receptor protein interactions. *Methods in Molecular Biology*, 400, 531–542. doi:10.1007/978-1-59745-519-0\_36.

Antollini, S.S., Soto, M.A., Bonini de Romanelli, I.C., Gutierrez-Merino, C., Sotomayor, P., & Barrantes, F.J. (1996). Physical state of bulk and protein-associated lipid in nicotinic acetylcholine receptor-rich membrane studied by laurdan generalized polarization and fluorescence energy transfer. *Biophysical Journal*, 70(3), 1275–1284. Retrieved from <http://www.ncbi.nlm.nih.gov/pubmed/0008785283>.

Arthur, J.R., Heinecke, K.A., & Seyfried, T.N. (2011). Filipin recognizes both GM1 and cholesterol in GM1 gangliosidosis mouse brain. *Journal of Lipid Research*, 52(7), 1345–1351. doi:10.1194/jlr.M012633.

Avramov, T.K., Vyenielo, D., Gomez-Blanco, J., Adinarayanan, S., Vargas, J., & Si, D. (2019). Deep learning for validating and estimating resolution of cryo-electron microscopy density maps. *Molecules*, 24(6), 1181. doi:10.3390/molecules24061181.

Azzi, A., Chance, B., Radda, G.K., & Lee, C.P. (1969). A fluorescence probe of energy-dependent structure changes in fragmented membranes. *Proceedings of the National Academy of Sciences of the United States of America*, 62(2), 612–619. doi:10.1073/pnas.62.2.612.

Bacalum, M., Zorilă, B., & Radu, M. (2013). Fluorescence spectra decomposition by asymmetric functions: Laurdan spectrum revisited. *Analytical Biochemistry*, 440(2), 123–129. doi:10.1016/j.ab.2013.05.031.

Bacia, K., Scherfeld, D., Kahya, N., & Schwille, P. (2004). Fluorescence correlation spectroscopy relates rafts in model and native membranes. *Biophysical Journal*, 87(2), 1034–1043. doi:10.1529/biophysj.104.040519.

- Bagatolli, L.A. (2006). To see or not to see: Lateral organization of biological membranes and fluorescence microscopy. *Biochimica et Biophysica Acta*, 1758(10), 1541–1556. Retrieved from <http://www.ncbi.nlm.nih.gov/pubmed/16854370>.
- Bagatolli, L.A., & Gratton, E. (1999). Two-photon fluorescence microscopy observation of shape changes at the phase transition in phospholipid giant unilamellar vesicles. *Biophysical Journal*, 77(4), 2090–2101. Retrieved from <http://www.ncbi.nlm.nih.gov/pubmed/10512829>.
- Bagatolli, L.A., Gratton, E., & Fidelio, G.D. (1998). Water dynamics in glycosphingolipid aggregates studied by LAURDAN fluorescence. *Biophysical Journal*, 75(1), 331–341.
- Bagatolli, L.A., Maggio, B., Aguilar, F., Sotomayor, C.P., & Fidelio, G.D. (1997). Laurdan properties in glycosphingolipid-phospholipid mixtures: A comparative fluorescence and calorimetric study. *Biochimica et Biophysica Acta*, 1325(1), 80–90.
- Bagatolli, L.A., Parasassi, T., & Gratton, E. (2000). Giant phospholipid vesicles: Comparison among the whole lipid sample characteristics using different preparation methods: A two photon fluorescence microscopy study. *Chemistry and Physics of Lipids*, 105(2), 135–147. Retrieved from <http://www.ncbi.nlm.nih.gov/pubmed/10823462>.
- Barreales, E.G., Payero, T.D., de Pedro, A., & Aparicio, J.F. (2018). Phosphate effect on filipin production and morphological differentiation in *Streptomyces filipinensis* and the role of the PhoP transcription factor. *PLoS One*, 13(12), e0208278. doi:10.1371/journal.pone.0208278.
- Bates, M., Huang, B., Dempsey, G.T., & Zhuang, X. (2007). Multicolor super-resolution imaging with photo-switchable fluorescent probes. *Science*, 317, 1749–1753. Retrieved from <https://doi.org/10.1126/science.1146598>.
- Bates, M., Huang, B., & Zhuang, X. (2008). Super-resolution microscopy by nanoscale localization of photo-switchable fluorescent probes. *Current Opinion in Chemical Biology*, 12(5), 505–514. Retrieved from <http://www.ncbi.nlm.nih.gov/pubmed/18809508>.
- Baumgart, T., Hammond, A.T., Sengupta, P., Hess, S.T., Holowka, D.A., & Baird, B.A., et al. (2007). Large-scale fluid/fluid phase separation of proteins and lipids in giant plasma membrane vesicles. *Proceedings of the National Academy of Sciences of the United States of America*, 104(9), 3165–3170. doi:10.1073/pnas.0611357104.
- Baumgarten, C.M., Makielski, J.C., & Fozzard, H.A. (1991). External site for local anesthetic block of cardiac Na<sup>+</sup> channels. *Journal of Molecular and Cellular Cardiology*, 23(Suppl. 1), 85–93.
- Belov, V.N., Wurm, C.A., Boyarskiy, V.P., Jakobs, S., & Hell, S.W. (2010). Rhodamines NN: A novel class of caged fluorescent dyes. *Angewandte Chemie International Edition in English*. Retrieved from <http://www.ncbi.nlm.nih.gov/pubmed/20391447>.
- Ben-Yashar, V., & Barenholz, Y. (1989). The interaction of cholesterol and cholest-4-en-3-one with dipalmitoylphosphatidylcholine. Comparison based on the use of three fluorophores. *Biochimica et Biophysica Acta*, 985, 271–278.
- Betzig, E. (2015). Single molecules, cells, and super-resolution optics (nobel lecture). *Angewandte Chemie (International Edition in English)*. doi:10.1002/anie.201501003.
- Bongiovanni, M.N., Godet, J., Horrocks, M.H., Tosatto, L., Carr, A.R., & Wirthensohn, D.C., et al. (2016). Multi-dimensional super-resolution imaging enables surface hydrophobicity mapping. *Nature*

Börnig, H., & Geyer, G. (1974). Staining of cholesterol with the fluorescent antibiotic “filipin”. *Acta Histochemica*, 50(1), 110–115.

Bossi, M., Belov, V., Polyakova, S., & Hell, S.W. (2006). Reversible red fluorescent molecular switches. *Angewandte Chemie (International Ed. in English)*, 45(44), 7462–7465. Retrieved from <http://www.ncbi.nlm.nih.gov/pubmed/17042053>.

Boyarskiy, V.P., Belov, V.N., Medda, R., Hein, B., Bossi, M., & Hell, S.W. (2008). Photostable, amino reactive and water-soluble fluorescent labels based on sulfonated rhodamine with a rigidized xanthen fragment. *Chemistry*, 14(6), 1784–1792. Retrieved from <http://www.ncbi.nlm.nih.gov/pubmed/18058955>.

Brent, R., & Boucheron, L. (2018). Deep learning to predict microscope images. *Nature Methods*, 15(11), 868–870. doi:10.1038/s41592-018-0194-9.

Brewer, J., de la Serna, J.B., Wagner, K., & Bagatolli, L.A. (2010). Multiphoton excitation fluorescence microscopy in planar membrane systems. *Biochimica et Biophysica Acta*, 1798(7), 1301–1308. Retrieved from <http://www.ncbi.nlm.nih.gov/pubmed/20226161>.

Brown, M.S., & Goldstein, J.L. (1984). How LDL receptors influence cholesterol and atherosclerosis. *Scientific American*, 251, 52–60.

Butkevich, A.N., Bossi, M.L., Lukinavičius, G., & Hell, S.W. (2019). Triarylmethane fluorophores resistant to oxidative photobleaching. *Journal of the American Chemical Society*, 141(2), 981–989. doi:10.1021/jacs.8b11036.

Butkevich, A.N., Yu, G., Mitronova, S.C., Klocke, J.L., Kamin, D., & Meineke, N.H., et al. (2016). Fluorescent rhodamines and fluorogenic carbopyronines for super-resolution STED microscopy in living cells. *Angewandte Chemie (International Ed. in English)*, 55, 3290–3294. Retrieved from <https://doi.org/10.1002/anie.201511018>.

Buwaneka, P., Ralko, A., Liu, S.-L., & Cho, W. (2021). Evaluation of the available cholesterol concentration in the inner leaflet of the plasma membrane of mammalian cells. *Journal of Lipid Research*, 62, 100084. doi:10.1016/j.jlr.2021.100084.

Q6

Calafut, T.M., Dix, J.A., & Verkman, A.S. (1989). Fluorescence depolarization of *cis*- and *trans*-parinaric acids in artificial and red cell membranes resolved by a double hindered rotational model. *Biochemistry*, 28, 5051–5058.

Carquin, M., Pollet, H., Veiga-da-Cunha, M., Cominelli, A., Van Der Smissen, P., & N’Kuli, F., et al. (2014). Endogenous sphingomyelin segregates into submicrometric domains in the living erythrocyte membrane. *Journal of Lipid Research*, 55(7), 1331–1342. doi:10.1194/jlr.M048538.

Carravilla, P., Dasgupta, A., Zhurgenbayeva, G., Danylchuk, D.I., Klymchenko, A.S., & Sezgin, E., et al. (2021). STED super-resolution imaging of membrane packing and dynamics by exchangeable polarity-sensitive dyes. *bioRxiv*. doi:10.1101/2021.06.05.446432.

Castanho, M.A.R.B., Coutinho, A., & Prieto, M.J.E. (1992). Absorption and fluorescence spectra of polyene antibiotics in the presence of cholesterol. *The Journal of Biological Chemistry*, 267(1), 204–209.

Castanho, M., & Prieto, M. (1995). Filipin fluorescence quenching by spin-labeled probes: Studies in aqueous solution and in a membrane model system. *Biophysical Journal*, 69(1), 155–168. doi:10.1016/S0006-



Castanho, M., Prieto, M., & Acuña, A.U. (1996). The transverse location of the fluorescent probe *trans*-parinaric acid in lipid bilayers. *Biochimica Biophysica Acta Bio-Membranes*, 1279, 164–168.

Cater, B.R., Chapman, D., Hawes, S.M., & Saville, J. (1974). Lipid phase transitions and drug interactions. *Biochimica et Biophysica Acta*, 363(1), 54–69. doi:10.1016/0005-2736(74)90006-6.

Chattopadhyay, A. (2003). Exploring membrane organization and dynamics by the wavelength-selective fluorescence approach. *Chemistry and Physics of Lipids*, 122(1–2), 3–17. Retrieved from <http://www.ncbi.nlm.nih.gov/pubmed/12598034>.

Chattopadhyay, A., Biswas, S.C., Rukmini, R., Saha, S., & Samanta, A. (2021). Lack of environmental sensitivity of a naturally occurring fluorescent analog of cholesterol. *Journal of Fluorescence*, 31, 1401–1407. doi:10.1007/s10895-021-02767-4.

Chattopadhyay, A., & Mukherjee, S. (1993). Fluorophore environments in membrane-bound probes: A red edge excitation shift study. *Biochemistry*, 32(14), 3804–3811. doi:10.1021/bi00065a037.

Chazotte, B. (2011). Labeling the plasma membrane with TMA-DPH. *Cold Spring Harbor Protocols*, 2011(5). doi:10.1101/pdb.prot5622.

Christiansen, E.M., Yang, S.J., Ando, D.M., Javaherian, A., Skibinski, G., & Lipnick, S., et al. (2018). In silico labeling: Predicting fluorescent labels in unlabeled images. *Cell*, 173(3), 792–803.e719. doi:10.1016/j.cell.2018.03.040.

Cogan, U., Shinitzky, M., Weber, G., & Nishida, T. (1973). Microviscosity and order in the hydrocarbon region of phospholipid and phospholipid-cholesterol dispersions determined with fluorescent probes. *Biochemistry*, 12(3), 521–528. doi:10.1021/bi00727a026.

Connor, O.D., Byrne, A., Berselli, G.B., Long, C., & Keyes, T.E. (2019). Mega-stokes pyrene ceramide conjugates for STED imaging of lipid droplets in live cells. *Analyst*, 144(5), 1608–1621. doi:10.1039/c8an02260g.

Courtney, K.C., Pezeshkian, W., Raghupathy, R., Zhang, C., Darbyson, A., & Ipsen, J.H., et al. (2018). C24 sphingolipids govern the transbilayer asymmetry of cholesterol and lateral organization of model and live-cell plasma membranes. *Cell Reports*, 24(4), 1037–1049. doi:10.1016/j.celrep.2018.06.104.

Cuevas Arenas, R., Danielczak, B., Martel, A., Porcar, L., Breyton, C., & Ebel, C., et al. (2017). Fast collisional lipid transfer among polymer-bounded nanodiscs. *Scientific Reports*, 7, 45875. doi:10.1038/srep45875.

Danylchuk, D.I., Moon, S., Xu, K., & Klymchenko, A.S. (2019). Switchable solvatochromic probes for live-cell super-resolution imaging of plasma membrane organization. *Angewandte Chemie (International Ed. in English)*, 58(42), 14920–14924. doi:10.1002/anie.201907690.

Das, A., Brown, M.S., Anderson, D.D., Goldstein, J.L., & Radhakrishnan, A. (2014). Three pools of plasma membrane cholesterol and their relation to cholesterol homeostasis. *eLife*, 3, e02882. doi:10.7554/eLife.02882.

De Craene, J.O., Bertazzi, D.L., Bär, S., & Friant, S. (2017). Phosphoinositides, major actors in membrane trafficking and lipid signaling pathways. *International Journal of Molecular Sciences*, 18(3). doi:10.3390/ijms18030634.

- de Saint-Jean, M., Delfosse, V., Douguet, D., Chicanne, G., Payrastré, B., & Bourguet, W., et al. (2011). Osh4p exchanges sterols for phosphatidylinositol 4-phosphate between lipid bilayers. *The Journal of Cell Biology*, 195(6), 965–978. doi:10.1083/jcb.201104062.
- Demchenko, A.P., Mely, Y., Duportail, G., & Klymchenko, A.S. (2009). Monitoring biophysical properties of lipid membranes by environment-sensitive fluorescent probes. *Biophysical Journal*, 96(9), 3461–3470. Retrieved from <http://www.ncbi.nlm.nih.gov/pubmed/19413953>.
- Dempsey, G.T., Vaughan, J.C., Chen, K.H., Bates, M., & Zhuang, X. (2011). Evaluation of fluorophores for optimal performance in localization-based super-resolution imaging. *Nature Methods*, 8, 1027–1036. Retrieved from <https://doi.org/10.1038/nmeth.1768>.
- Dietrich, C., Bagatolli, L.A., Volovyk, Z.N., Thompson, N.L., Levi, M., & Jacobson, K., et al. (2001). Lipid rafts reconstituted in model membranes. *Biophysical Journal*, 80(3), 1417–1428. Retrieved from <http://www.ncbi.nlm.nih.gov/pubmed/11222302>.
- Dirix, L., Kennes, K., Fron, E., Debyser, Z., van der Auweraer, M., & Hofkens, J., et al. (2018). Photoconversion of far-red organic dyes: Implications for multicolor super-resolution imaging. *ChemPhotoChem*, 2(5), 433–441. <https://doi.org/10.1002/cptc.201700216>.
- do Canto, A., Robalo, J.R., Santos, P.D., Carvalho, A.J.P., Ramalho, J.P.P., & Loura, L.M.S. (2016). Diphenylhexatriene membrane probes DPH and TMA-DPH: A comparative molecular dynamics simulation study. *Biochimica et Biophysica Acta*, 1858(11), 2647–2661. doi:10.1016/j.bbamem.2016.07.013.
- Dong, B., Almassalha, L., Urban, B.E., Nguyen, T.-Q., Khuon, S., & Chew, T.-L., et al. (2016). Super-resolution spectroscopic microscopy via photon localization. *Nature Communications*, 7. doi:10.1038/ncomms12290.
- Drabikowski, W., Lagwińska, E., & Sarzala, M.G. (1973). Filipin as a fluorescent probe for the location of cholesterol in the membranes of fragmented sarcoplasmic reticulum. *Biochimica et Biophysica Acta*, 291(1), 61–70. doi:10.1016/0005-2736(73)90060-6.
- Eggeling, C. (2015). Super-resolution optical microscopy of lipid plasma membrane dynamics. *Essays in Biochemistry*, 57, 69–80. doi:10.1042/bse0570069.
- Eggeling, C., Widengren, J., Rigler, R., & Seidel, C.A.M. (1998). Photobleaching of fluorescent dyes under conditions used for single-molecule detection: Evidence of two-step photolysis. *Analytical Chemistry*, 70(13), 2651–2659.
- Epanand, R.F., Kraayenhof, R., Sterk, G.J., Sang, H.W.W.F., & Epanand, R.M. (1996). Fluorescent probes of membrane surface properties. *Biochimica et Biophysica Acta. Bio-Membranes*, 1284(2), 191–195.
- Ercan, B., Naito, T., Koh, D.H.Z., Dharmawan, D., & Saheki, Y. (2021). Molecular basis of accessible plasma membrane cholesterol recognition by the GRAM domain of GRAMD1b. *The EMBO Journal*, 40(6), e106524. doi:10.15252/embj.2020106524.
- Fereidouni, F., Bader, A.N., & Gerritsen, H.C. (2012). Spectral phasor analysis allows rapid and reliable unmixing of fluorescence microscopy spectral images. *Optics Express*, 20(12), 12729–12741. doi:10.1364/oe.20.012729.
- Fernández-Luna, V., Coto, P.B., & Costa, R.D. (2018). When fluorescent proteins meet white light-emitting diodes. *Angewandte Chemie (International Ed. in English)*, 57(29), 8826–8836. doi:10.1002/anie.201711433.

Ferretti, G., Tangorra, A., Zolese, G., & Curatola, G. (1993). Properties of a phosphatidylcholine derivative of diphenyl hexatriene (DPH-PC) in lymphocyte membranes. A comparison with DPH and the cationic derivative TMA-DPH using static and dynamic fluorescence. *Membrane Biochemistry*, 10(1), 17–27. doi:10.3109/09687689309150249.

Filipe, H.A.L., Pokorná, Š., Hof, M., Amaro, M., & Loura, L.M.S. (2019). Orientation of nitro-group governs the fluorescence lifetime of nitrobenzoxadiazole (NBD)-labeled lipids in lipid bilayers. *Physical Chemistry Chemical Physics*, 21(4), 1682–1688. doi:10.1039/c8cp06064a.

Fiorini, R., Curatola, G., Kantar, A., Giorgi, P.L., & Gratton, E. (1993). Use of Laurdan fluorescence in studying plasma membrane organization of polymorphonuclear leukocytes during the respiratory burst. *Photochemistry and Photobiology*, 57, 438–441.

Flanagan, J.J., Tweten, R.K., Johnson, A.E., & Heuck, A.P. (2009). Cholesterol exposure at the membrane surface is necessary and sufficient to trigger perfringolysin O binding. *Biochemistry*, 48(18), 3977–3987. doi:10.1021/bi9002309.

Fujimoto, T., Hayashi, M., Iwamoto, M., & Ohno-Iwashita, Y. (1997). Crosslinked plasmalemmal cholesterol is sequestered to caveolae: Analysis with a new cytochemical probe. *The Journal of Histochemistry and Cytochemistry*, 45(9), 1197–1205.

Gallegos, A.M., McIntosh, A.L., Atshaves, B.P., & Schroeder, F. (2004). Structure and cholesterol domain dynamics of an enriched caveolae/raft isolate. *The Biochemical Journal*, 382(Pt. 2), 451–461. doi:10.1042/bj20031562.

Garvik, O., Benediktson, P., Simonsen, A.C., Ipsen, J.H., & Wüstner, D. (2009). The fluorescent cholesterol analog dehydroergosterol induces liquid-ordered domains in model membranes. *Chemistry and Physics of Lipids*, 159(2), 114–118. doi:10.1016/j.chemphyslip.2009.03.002.

Gaus, K., Gratton, E., Kable, E.P., Jones, A.S., Gelissen, I., & Kritharides, L., et al. (2003). Visualizing lipid structure and raft domains in living cells with two-photon microscopy. *Proceedings of the National Academy of Sciences of the United States of America*, 100(26), 15554–15559. Retrieved from <http://www.ncbi.nlm.nih.gov/pubmed/14673117>.

Gaus, K., Zech, T., & Harder, T. (2006). Visualizing membrane microdomains by Laurdan 2-photon microscopy. *Molecular Membrane Biology*, 23(1), 41–48. Retrieved from <http://www.ncbi.nlm.nih.gov/pubmed/16611579>.

Geyer, G., & Börmig, H. (1975). “Filipin”—A histochemical fluorochrome for cholesterol. *Acta Histochemica. Supplementband*, 15, 207–212.

Giang, H., & Schick, M. (2016). On the puzzling distribution of cholesterol in the plasma membrane. *Chemistry and Physics of Lipids*, 199, 35–38. doi:10.1016/j.chemphyslip.2015.12.002.

Godement, P., Vanselow, J., Thanos, S., & Bonhoeffer, F. (1987). A study in developing visual systems with a new method of staining neurones and their processes in fixed tissue. *Development*, 101(4), 697–713.

Golfetto, O., Hinde, E., & Gratton, E. (2013). Laurdan fluorescence lifetime discriminates cholesterol content from changes in fluidity in living cell membranes. *Biophysical Journal*, 104(6), 1238–1247. doi:10.1016/j.bpj.2012.12.057.

Golfetto, O., Hinde, E., & Gratton, E. (2015). The Laurdan spectral phasor method to explore membrane micro-heterogeneity and lipid domains in live cells. *Methods in Molecular Biology*, 1232, 273–290.

Gould, T.J., Hess, S.T., & Bewersdorf, J. (2012). Optical nanoscopy: From acquisition to analysis. *Annual Review of Biomedical Engineering*, 14, 231–254. doi:10.1146/annurev-bioeng-071811-150025.

Grimm, J.B., English, B.P., Chen, J., Slaughter, J.P., Zhang, Z., & Revyakin, A., et al. (2015). A general method to improve fluorophores for live-cell and single-molecule microscopy. *Nature Methods*, 12(3), 244–250. doi:10.1038/nmeth.3256. <http://www.nature.com/nmeth/journal/v12/n3/abs/nmeth.3256.html#supplementary-information>.

Grimm, J.B., English, B.P., Choi, H., Muthusamy, A.K., Mehl, B.P., & Dong, P., et al. (2016). Bright photoactivatable fluorophores for single-molecule imaging. *Nature Methods*, 13(12), 985–988. doi:10.1038/nmeth.4034. <http://www.nature.com/nmeth/journal/v13/n12/abs/nmeth.4034.html#supplementary-information>.

Gunther, G., Malacrida, L., Jameson, D.M., Gratton, E., & Sánchez, S.A. (2021). LAURDAN since Weber: The quest for visualizing membrane heterogeneity. *Accounts of Chemical Research*, 54(4), 976–987. doi:10.1021/acs.accounts.0c00687.

Ha, T., & Tinnefeld, P. (2012). Photophysics of fluorescent probes for single-molecule biophysics and super-resolution imaging. *Annual Review of Physical Chemistry*, 63, 595–617. doi:10.1146/annurev-physchem-032210-103340.

Hale, J.E., & Schroeder, F. (1982). Asymmetric transbilayer distribution of sterol across plasma membranes determined by fluorescence quenching of dehydroergosterol. *European Journal of Biochemistry*, 122, 649–661.

Hammond, G.R., Machner, M.P., & Balla, T. (2014). A novel probe for phosphatidylinositol 4-phosphate reveals multiple pools beyond the Golgi. *The Journal of Cell Biology*, 205(1), 113–126. doi:10.1083/jcb.201312072.

Hao, M., Lin, S.X., Karylowski, O.J., Wustner, D., McGraw, T.E., & Maxfield, F.R. (2002). Vesicular and non-vesicular sterol transport in living cells. The endocytic recycling compartment is a major sterol storage organelle. *The Journal of Biological Chemistry*, 277(1), 609–617. Retrieved from <http://www.ncbi.nlm.nih.gov/pubmed/11682487>.

Hao, M., Mukherjee, S., & Maxfield, F.R. (2001). Cholesterol depletion induces large scale domain segregation in living cell membranes. *Proceedings of the National Academy of Sciences of the United States of America*, 98(23), 13072–13077. Retrieved from <http://www.ncbi.nlm.nih.gov/pubmed/11698680>.

Hayashi, M., Shimada, Y., Inomata, M., & Ohno-Iwashita, Y. (2006). Detection of cholesterol-rich microdomains in the inner leaflet of the plasma membrane. *Biochemical and Biophysical Research Communications*, 351(3), 713–718. doi:10.1016/j.bbrc.2006.10.088.

Heider, E.C., Barhoum, M., Peterson, E.M., Schaefer, J., & Harris, J.M. (2010). Identification of single fluorescent labels using spectroscopic microscopy. *Applied Spectroscopy*, 64(1), 37–45. doi:10.1366/000370210790572034.

Heino, S., Lusa, S., Somerharju, P., Ehnholm, C., Olkkonen, V.M., & Ikonen, E. (2000). Dissecting the role of the golgi complex and lipid rafts in biosynthetic transport of cholesterol to the cell surface. *Proceedings of the National Academy of Sciences of the United States of America*, 97(15), 8375–8380. Retrieved from <http://www.ncbi.nlm.nih.gov/pubmed/10890900>.

- Helgadottir, S., Midtvedt, B., Pineda, J., Sabirsh, A., Adiels, C.B., & Romeo, S., et al. (2021). Extracting quantitative biological information from bright-field cell images using deep learning. *Biophysics Reviews*, 2(3), 031401. doi:10.1063/5.0044782.
- Hell, S.W. (2015). Nanoscopy with focused light (nobel lecture). *Angewandte Chemie (International Ed. in English)*. doi:10.1002/anie.201504181.
- Hell, S.W., & Wichmann, J. (1994). Breaking the diffraction resolution limit by stimulated emission: Stimulated-emission-depletion fluorescence microscopy. *Optics Letters*, 19, 780–782. Retrieved from <https://doi.org/10.1364/OL.19.000780>.
- Helmerich, D.A., Beliu, G., Matikonda, S.S., Schnermann, M.J., & Sauer, M. (2021). Photobleuing of organic dyes can cause artifacts in super-resolution microscopy. *Nature Methods*. doi:10.1038/s41592-021-01061-2.
- Henriques, R., Griffiths, C., Hesper Rego, E., & Mhlanga, M.M. (2011). PALM and STORM: Unlocking live-cell super-resolution. *Biopolymers*, 95(5), 322–331. doi:10.1002/bip.21586.
- Hense, A., Prunsche, B., Gao, P., Ishitsuka, Y., Nienhaus, K., & Nienhaus, G.U. (2015). Monomeric Garnet, a far-red fluorescent protein for live-cell STED imaging. *Scientific Reports*, 5, 18006. doi:10.1038/srep18006.
- Hess, S.T., Girirajan, T.P., & Mason, M.D. (2006). Ultra-high resolution imaging by fluorescence photoactivation localization microscopy. *Biophysics Journal*, 91(11), 4258–4272. Retrieved from <http://www.ncbi.nlm.nih.gov/pubmed/16980368>.
- Honig, M.G., & Hume, R.I. (1989). Dil and diO: Versatile fluorescent dyes for neuronal labelling and pathway tracing. *Trends in Neurosciences*, 12(9), 333–335. 340-331.
- Honigmann, A., Mueller, V., Hell, S.W., & Eggeling, C. (2013). STED microscopy detects and quantifies liquid phase separation in lipid membranes using a new far-red emitting fluorescent phosphoglycerolipid analogue. *Faraday Discussions*, 161, 77–89. discussion 113–150 <https://doi.org/10.1039/c2fd20107k>.
- Hullin-Matsuda, F., & Kobayashi, T. (2007). Monitoring the distribution and dynamics of signaling microdomains in living cells with lipid-specific probes. *Cellular and Molecular Life Sciences*, 64(19–20), 2492–2504. doi:10.1007/s00018-007-7281-x.
- Ikonen, E. (2008). Cellular cholesterol trafficking and compartmentalization. *Nature Reviews Molecular Cell Biology*, 9(2), 125–138. Retrieved from <http://www.ncbi.nlm.nih.gov/pubmed/18216769>.
- Illinger, D., Duportail, G., Poirel-Morales, N., Gerard, D., & Kuhry, J.-G. (1995). A comparison of the fluorescence properties of TMA-DPH as a probe for plasma membrane and for endocytic membrane. *Biochimica et Biophysica Acta*, 1239, 58–66.
- Illinger, D., Italiano, L., Beck, J.-P., Waltzinger, C., & Kuhry, J.-G. (1993). Comparative evolution of endocytosis levels and of the cell surface area during the L929 cell cycle: A fluorescence study with TMA-DPH. *Biology of the Cell*, 79, 265–268.
- Illinger, D., Poindron, P., & Kuhry, J.-G. (1991). Fluid phase endocytosis investigated by fluorescence with trimethylamino-diphenylhexatriene in L929 cells; the influence of temperature and of cytoskeleton depolymerizing drugs. *Biology of the Cell*, 73, 131–138.
- Im, Y.J., Raychaudhuri, S., Prinz, W.A., & Hurley, J.H. (2005). Structural mechanism for sterol sensing and transport by OSBP-related proteins. *Nature*, 437(7055), 154–158. doi:10.1038/nature03923.

- Jacobson, K., Mouritsen, O.G., & Anderson, R.G. (2007). Lipid rafts: At a crossroad between cell biology and physics. *Nature Cell Biology*, 9(1), 7–14. doi:10.1038/ncb0107-7.
- Jacobson, K., & Wobschall, D. (1974). Rotation of fluorescent probes localized within lipid bilayer membranes. *Chemistry and Physics of Lipids*, 12(2), 117–131. doi:10.1016/0009-3084(74)90049-8.
- Jameson, D.M., Gratton, E., & Hall, R.D. (1984). The measurement and analysis of heterogeneous emissions by multifrequency phase and modulation fluorometry. *Applied Spectroscopy Reviews*, 20, 55–106.
- Jamshad, M., Lin, Y.P., Knowles, T.J., Parslow, R.A., Harris, C., & Wheatley, M., et al. (2011). Surfactant-free purification of membrane proteins with intact native membrane environment. *Biochemical Society Transactions*, 39(3), 813–818. doi:10.1042/bst0390813.
- Jiang, Y.W., Guo, H.Y., Chen, Z., Yu, Z.W., Wang, Z., & Wu, F.G. (2016). In situ visualization of lipid raft domains by fluorescent glycol chitosan derivatives. *Langmuir*, 32(26), 6739–6745. doi:10.1021/acs.langmuir.6b00193.
- Jin, L., Millard, A.C., Wuskell, J.P., Clark, H.A., & Loew, L.M. (2005). Cholesterol-enriched lipid domains can be visualized by di-4-ANEPPDHQ with linear and nonlinear optics. *Biophysical Journal*, 89(1), L04–L06. Retrieved from <http://www.ncbi.nlm.nih.gov/pubmed/15879475>.
- Jin, L., Millard, A.C., Wuskell, J.P., Dong, X., Wu, D., & Clark, H.A., et al. (2006). Characterization and application of a new optical probe for membrane lipid domains. *Biophysical Journal*, 90(7), 2563–2575. Retrieved from <http://www.ncbi.nlm.nih.gov/pubmed/16415047>.
- Juhasz, J., Davis, J.H., & Sharom, F.J. (2010). Fluorescent probe partitioning in giant unilamellar vesicles of “lipid raft” mixtures. *The Biochemical Journal*, 430(3), 415–423. doi:10.1042/bj20100516.
- Jungmann, R. (2014). Multiplexed 3D cellular super-resolution imaging with DNA-PAINT and exchange-PAINT. *Nature Methods*, 11, 313–318. Retrieved from <https://doi.org/10.1038/nmeth.2835>.
- Kahya, N., Scherfeld, D., Bacia, K., Poolman, B., & Schwille, P. (2003). Probing lipid mobility of raft-exhibiting model membranes by fluorescence correlation spectroscopy. *The Journal of Biological Chemistry*, 278(30), 28109–28115. Retrieved from <http://www.ncbi.nlm.nih.gov/pubmed/12736276>.
- Kahya, N., Scherfeld, D., & Schwille, P. (2005). Differential lipid packing abilities and dynamics in giant unilamellar vesicles composed of short-chain saturated glycerol-phospholipids, sphingomyelin and cholesterol. *Chemistry and Physics of Lipids*, 135(2), 169–180. Retrieved from <http://www.ncbi.nlm.nih.gov/pubmed/15869751>.
- Kaiser, R.D., & London, E. (1998). Location of diphenylhexatriene (DPH) and its derivatives within membranes: Comparison of different fluorescence quenching analyses of membrane depth. *Biochemistry*, 37(22), 8180–8190. doi:10.1021/bi980064a.
- Kamerbeek, C.B., Borroni, V., Pediconi, M.F., Sato, S.B., Kobayashi, T., & Barrantes, F.J. (2013). Antibody-induced acetylcholine receptor clusters inhabit liquid-ordered and liquid-disordered domains. *Biophysical Journal*, 105(7), 1601–1611. doi:10.1016/j.bpj.2013.08.039.
- Kanfer, G., Sarraf, S.A., Maman, Y., Baldwin, H., Dominguez-Martin, E., & Johnson, K.R., et al. (2021). Image-based pooled whole-genome CRISPRi screening for subcellular phenotypes. *The Journal of Cell Biology*, 220(2). doi:10.1083/jcb.202006180.

- Karlsen, M.L., Bruhn, D.S., Pezeshkian, W., & Khandelia, H. (2021). Long chain sphingomyelin depletes cholesterol from the cytoplasmic leaflet in asymmetric lipid membranes. *RSC Advances*, 11(37), 22677–22682. doi:10.1039/D1RA01464A.
- Kassas, N., Tanguy, E., Thahouly, T., Fouillen, L., Heintz, D., & Chasserot-Golaz, S., et al. (2017). Comparative characterization of phosphatidic acid sensors and their localization during frustrated phagocytosis. *The Journal of Biological Chemistry*, 292(10), 4266–4279. doi:10.1074/jbc.M116.742346.
- Kay, J.G., & Fair, G.D. (2019). Distribution, dynamics and functional roles of phosphatidylserine within the cell. *Cell Communication and Signaling: CCS*, 17(1), 126. doi:10.1186/s12964-019-0438-z.
- Kier, A.B., Sweet, W.D., Cowlen, M.S., & Schroeder, F. (1986). Regulation of transbilayer distribution of a fluorescent sterol in tumor cell plasma membranes. *Biochimica et Biophysica Acta*, 861(2), 287–301.
- Kinoshita, M., Suzuki, K.G., Matsumori, N., Takada, M., Ano, H., & Morigaki, K., et al. (2017). Raft-based sphingomyelin interactions revealed by new fluorescent sphingomyelin analogs. *The Journal of Cell Biology*, 216(4), 1183–1204. doi:10.1083/jcb.201607086.
- Kinsky, S.C., Luse, S.A., Zopf, D., Van Deenen, L.L.M., & Haxby, J. (1967). Interaction of filipin and derivatives with erythrocyte membranes and lipid dispersions: Electron microscopic observations. *Biochimica et Biophysica Acta (BBA) - Biomembranes*, 135(5), 844–861. doi:10.1016/0005-2736(67)90055-7.
- Kishimoto, T., Ishitsuka, R., & Kobayashi, T. (2016). Detectors for evaluating the cellular landscape of sphingomyelin- and cholesterol-rich membrane domains. *Biochimica et Biophysica Acta (BBA) - Molecular and Cell Biology of Lipids*, 1861(8, Part B), 812–829. <https://doi.org/10.1016/j.bbalip.2016.03.013>.
- Klymchenko, A.S. (2017). Solvatochromic and fluorogenic dyes as environment-sensitive probes: Design and biological applications. *Accounts of Chemical Research*, 50(2), 366–375. doi:10.1021/acs.accounts.6b00517.
- Knowles, T.J., Finka, R., Smith, C., Lin, Y.P., Dafforn, T., & Overduin, M. (2009). Membrane proteins solubilized intact in lipid containing nanoparticles bounded by styrene maleic acid copolymer. *Journal of the American Chemical Society*, 131(22), 7484–7485. doi:10.1021/ja810046q.
- Kobayashi, T., & Menon, A.K. (2018). Transbilayer lipid asymmetry. *Current Biology*, 28(8), R386–R391. doi:10.1016/j.cub.2018.01.007.
- Korlach, J., Schwille, P., Webb, W.W., & Feigenson, G.W. (1999). Characterization of lipid bilayer phases by confocal microscopy and fluorescence correlation spectroscopy. *Proceedings of the National Academy of Sciences of the United States of America*, 96(15), 8461–8466. Retrieved from <http://www.ncbi.nlm.nih.gov/pubmed/10411897>.
- Kremers, G.J., Gilbert, S.G., Cranfill, P.J., Davidson, M.W., & Piston, D.W. (2011). Fluorescent proteins at a glance. *Journal of Cell Science*, 124(Pt. 2), 157–160. doi:10.1242/jcs.072744.
- Krizhevsky, A., Sutskever, I., & Hinton, G.E. (2012). NIPS'12 Proc. 25th Int. Conf. Neural Inf. Process. Syst.
- Lange, Y., Swaisgood, M.H., Ramos, B.V., & Steck, T.L. (1989). Plasma membranes contain half the phospholipid and 90% of the cholesterol and sphingomyelin in cultured human fibroblasts. *The Journal of Biological Chemistry*, 264, 3786–3793.
- Lange, Y., Ye, J., & Steck, T.L. (2004). How cholesterol homeostasis is regulated by plasma membrane cholesterol in excess of phospholipids. *Proceedings of the National Academy of Sciences of the United States*

of the America, 101(32), 11664–11667. Retrieved from <http://www.ncbi.nlm.nih.gov/pubmed/15289597>.

Lemmon, M.A. (2008). Membrane recognition by phospholipid-binding domains. *Nature Reviews Molecular Cell Biology*, 9(2), 99–111. Retrieved from <http://www.ncbi.nlm.nih.gov/pubmed/18216767>.

Lesslauer, W., Cain, J.E., & Blasie, J.K. (1972). X-ray diffraction studies of lecithin bimolecular leaflets with incorporated fluorescent probes. *Proceedings of the National Academy of Sciences of the United States of America*, 69(6), 1499–1503. doi:10.1073/pnas.69.6.1499.

Levi, M., Wilson, P.V., Cooper, O.J., & Gratton, E. (1993). Lipid phases in renal brush border membranes revealed by Laurdan fluorescence. *Photochemistry and Photobiology*, 57, 420–425.

Li, Y.E., Wang, Y., Du, X., Zhang, T., Mak, H.Y., & Hancock, S.E., et al. (2021). TMEM41B and VMP1 are scramblases and regulate the distribution of cholesterol and phosphatidylserine. *Journal of Cell Biology*, 220(6). doi:10.1083/jcb.202103105.

Lim, C.Y., Davis, O.B., Shin, H.R., Zhang, J., Berdan, C.A., & Jiang, X., et al. (2019). ER-lysosome contacts enable cholesterol sensing by mTORC1 and drive aberrant growth signalling in Niemann-Pick type C. *Nature Cell Biology*, 21(10), 1206–1218. doi:10.1038/s41556-019-0391-5.

Lin, Q., & London, E. (2013). Transmembrane protein (perfringolysin o) association with ordered membrane domains (rafts) depends upon the raft-associating properties of protein-bound sterol. *Biophysical Journal*, 105(12), 2733–2742. doi:10.1016/j.bpj.2013.11.002.

Lin, Q., & London, E. (2015). Ordered raft domains induced by outer leaflet sphingomyelin in cholesterol-rich asymmetric vesicles. *Biophysical Journal*, 108(9), 2212–2222. <https://doi.org/10.1016/j.bpj.2015.03.056>.

Liu, X. (2019). ABC family transporters. *Advances in Experimental Medicine and Biology*, 1141, 13–100. doi:10.1007/978-981-13-7647-4\_2.

Liu, J., Chang, C.C., Westover, E.J., Covey, D.F., & Chang, T.Y. (2005). Investigating the allostereism of acyl-CoA:cholesterol acyltransferase (ACAT) by using various sterols: In vitro and intact cell studies. *The Biochemical Journal*, 391(Pt 2), 389–397. doi:10.1042/bj20050428.

Liu, S.L., Sheng, R., Jung, J.H., Wang, L., Stec, E., & O'Connor, M.J., et al. (2017). Orthogonal lipid sensors identify transbilayer asymmetry of plasma membrane cholesterol. *Nature Chemical Biology*, 13(3), 268–274. doi:10.1038/nchembio.2268.

Liu, Y., Su, Y., & Wang, X. (2013). Phosphatidic acid-mediated signaling. *Advances in Experimental Medicine and Biology*, 991, 159–176. doi:10.1007/978-94-007-6331-9\_9.

Loew, L.M., Cohen, L.B., Dix, J., Fluhler, E.N., Montana, V., & Salama, G., et al. (1992). A naphthyl analog of the aminostyryl pyridinium class of potentiometric membrane dyes shows consistent sensitivity in a variety of tissue, cell, and model membrane preparations. *The Journal of Membrane Biology*, 130, 1–10.

London, E. (2019). Membrane structure–function insights from asymmetric lipid vesicles. *Accounts of Chemical Research*. doi:10.1021/acs.accounts.9b00300.

Lorent, J.H., Levental, K.R., Ganesan, L., Rivera-Longworth, G., Sezgin, E., & Doktorova, M., et al. (2020). Plasma membranes are asymmetric in lipid unsaturation, packing and protein shape. *Nature Chemical Biology*, 16(6), 644–652. doi:10.1038/s41589-020-0529-6.



Lorizate, M., Terrones, O., Nieto-Garai, J.A., Rojo-Bartolomé, I., Ciceri, D., & Morana, O., et al. (2021). Super-resolution microscopy using a bioorthogonal-based cholesterol probe provides unprecedented capabilities for imaging nanoscale lipid heterogeneity in living cells. *Small Methods*, 2100430. <https://doi.org/10.1002/smt.202100430>.

Luzzati, V., Gulik-Krzywicki, T., Rivas, E., Reiss-Husson, F., & Rand, R.P. (1968). X-ray study of model systems: Structure of the lipid-water phases in correlation with the chemical composition of the lipids. *The Journal of General Physiology*, 51(5), 37–43.

Luzzati, V., & Husson, F. (1962). The structure of the liquid-crystalline phase of lipid-water systems. *The Journal of Cell Biology*, 12(2), 207–219. doi:10.1083/jcb.12.2.207.

Maekawa, M., & Fairn, G.D. (2015). Complementary probes reveal that phosphatidylserine is required for the proper transbilayer distribution of cholesterol. *Journal of Cell Science*, 128(7), 1422–1433. doi:10.1242/jcs.164715 %J Journal of Cell Science.

Makino, A., Abe, M., Ishitsuka, R., Murate, M., Kishimoto, T., & Sakai, S., et al. (2017). A novel sphingomyelin/cholesterol domain-specific probe reveals the dynamics of the membrane domains during virus release and in Niemann-Pick type C. *FASEB Journal: Official Publication of the Federation of American Societies for Experimental Biology*, 31(4), 1301–1322. doi:10.1096/fj.201500075R.

Man, Z., Cui, H., Lv, Z., Xu, Z., Wu, Z., & Wu, Y., et al. (2021). Organic nanoparticles-assisted low-power STED nanoscopy. *Nano Letters*. doi:10.1021/acs.nanolett.1c00161.

Manley, S., Gillette, J.M., Patterson, G.H., Shroff, H., Hess, H.F., & Betzig, E., et al. (2008). High-density mapping of single-molecule trajectories with photoactivated localization microscopy. *Nature Methods*, 5(2), 155–157. Retrieved from <http://www.ncbi.nlm.nih.gov/pubmed/18193054>.

Marsh, D. (1974). An interacting spin label study of lateral expansion in dipalmitoyllecithin-cholesterol bilayers. *Biochimica et Biophysica Acta*, 363(3), 373–386. doi:10.1016/0005-2736(74)90076-5.

Marshall, J.E., Faraj, B.H., Gingras, A.R., Lonnen, R., Sheikh, M.A., & El-Mezgueldi, M., et al. (2015). The crystal structure of pneumolysin at 2.0 Å resolution reveals the molecular packing of the pre-pore complex. *Scientific Reports*, 5, 13293. doi:10.1038/srep13293.

Matlashov, M.E., Shcherbakova, D.M., Alvelid, J., Baloban, M., Pennacchiotti, F., & Shemetov, A.A., et al. (2020). A set of monomeric near-infrared fluorescent proteins for multicolor imaging across scales. *Nature Communications*, 11(1), 239. doi:10.1038/s41467-019-13897-6.

Maxfield, F.R., & Tabas, I. (2005). Role of cholesterol and lipid organization in disease. *Nature*, 438(7068), 612–621. Retrieved from <http://www.ncbi.nlm.nih.gov/pubmed/16319881>.

Maxfield, F.R., & Wüstner, D. (2012). Analysis of cholesterol trafficking with fluorescent probes. *Methods in Cell Biology*, 108. doi:10.1016/b978-0-12-386487-1.00017-1.

Mayor, S., & Rao, M. (2004). Rafts: Scale-dependent, active lipid organization at the cell surface. *Traffic*, 5(4), 231–240. Retrieved from <http://www.ncbi.nlm.nih.gov/pubmed/15030564>.

McIntosh, A.L., Atshaves, B.P., Huang, H., Gallegos, A.M., Kier, A.B., & Schroeder, F. (2008). Fluorescence techniques using dehydroergosterol to study cholesterol trafficking. *Lipids*, 43(12), 1185–1208. doi:10.1007/s11745-008-3194-1.

- McIntosh, A.L., Atshaves, B.P., Huang, H., Gallegos, A.M., Kier, A.B., & Schroeder, F., et al. (2007). Multiphoton laser-scanning microscopy and spatial analysis of dehydroergosterol distributions on plasma membrane of living cells. In McIntosh, T.J. (Ed.), *Lipid Rafts* (pp. 85–105). Totowa, NJ: Humana Press.
- McIntyre, J.C., & Sleight, R.G. (1991). Fluorescence assay for phospholipid membrane asymmetry. *Biochemistry*, 30, 11819–11824.
- Mesmin, B., Pipalia, N.H., Lund, F.W., Ramlall, T.F., Sokolov, A., & Eliezer, D., et al. (2011). STARD4 abundance regulates sterol transport and sensing. *Molecular Biology of the Cell*, 22(21), 4004–4015. doi:10.1091/mbc.E11-04-0372.
- Miller, R.G. (1984). The use and abuse of filipin to localize cholesterol in membranes. *Cell Biology International Reports*, 8(7), 519–535. doi:10.1016/0309-1651(84)90050-x.
- Milles, S., Meyer, T., Scheidt, H.A., Schwarzer, R., Thomas, L., & Marek, M., et al. (2013). Organization of fluorescent cholesterol analogs in lipid bilayers—Lessons from cyclodextrin extraction. *Biochimica et Biophysica Acta*, 1828(8), 1822–1828. doi:10.1016/j.bbamem.2013.04.002.
- Mlodzianoski, M.J., Curthoys, N.M., Gunewardene, M.S., Carter, S., & Hess, S.T. (2016). Super-resolution imaging of molecular emission spectra and single molecule spectral fluctuations. *PLoS One*, 11(3), e0147506. doi:10.1371/journal.pone.0147506.
- Möbius, W., Ohno-Iwashita, Y., van Donselaar, E.G., Oorschot, V.M., Shimada, Y., & Fujimoto, T., et al. (2002). Immunoelectron microscopic localization of cholesterol using biotinylated and non-cytolytic perfringolysin O. *The Journal of Histochemistry and Cytochemistry*, 50(1), 43–55. doi:10.1177/002215540205000105.
- Moerner, W.E. (2015). Single-molecule spectroscopy, imaging, and photocontrol: Foundations for super-resolution microscopy (nobel lecture). *Angewandte Chemie (International Ed. in English)*. doi:10.1002/anie.201501949.
- Mondal, M., Mesmin, B., Mukherjee, S., & Maxfield, F.R. (2009). Sterols are mainly in the cytoplasmic leaflet of the plasma membrane and the endocytic recycling compartment in CHO cells. *Molecular Biology of the Cell*, 20(2), 581–588. Retrieved from <http://www.ncbi.nlm.nih.gov/pubmed/19019985>.
- Montes, L.R., Alonso, A., Goni, F.M., & Bagatolli, L.A. (2007). Giant unilamellar vesicles electroformed from native membranes and organic lipid mixtures under physiological conditions. *Biophysical Journal*, 93(10), 3548–3554. Retrieved from <http://www.ncbi.nlm.nih.gov/pubmed/17704162>.
- Montesano, R., Vassalli, P., & Orci, L. (1981). Structural heterogeneity of endocytic membranes in macrophages as revealed by the cholesterol probe, filipin. *Journal of Cell Science*, 51, 95–107.
- Moon, S., Yan, R., Kenny, S.J., Shyu, Y., Xiang, L., & Li, W., et al. (2017). Spectrally resolved, functional super-resolution microscopy reveals nanoscale compositional heterogeneity in live-cell membranes. *Journal of the American Chemical Society*, 139(32), 10944–10947. doi:10.1021/jacs.7b03846.
- Mukherjee, S., & Chattopadhyay, A. (1995). Wavelength-selective fluorescence as a novel tool to study organization and dynamics in complex biological systems. *Journal of Fluorescence*, 5, 237–245.
- Mukherjee, S., Zha, X.H., Tabas, I., & Maxfield, F.R. (1998). Cholesterol distribution in living cells: Fluorescence imaging using dehydroergosterol as a fluorescent cholesterol analog. *Biophysical Journal*, 75(4), 1915–1925.

Murate, M., Abe, M., Kasahara, K., Iwabuchi, K., Umeda, M., & Kobayashi, T. (2015). Transbilayer distribution of lipids at nano scale. *Journal of Cell Science*, 128(8), 1627–1638. doi:10.1242/jcs.163105.

Murate, M., & Kobayashi, T. (2016). Revisiting transbilayer distribution of lipids in the plasma membrane. *Chemistry and Physics of Lipids*, 194, 58–71. doi:10.1016/j.chemphyslip.2015.08.009.

Naito, T., & Saheki, Y. (1866). GRAMD1-mediated accessible cholesterol sensing and transport. *Biochimica et Biophysica Acta - Molecular and Cell Biology of Lipids*, 2021(8), 158957. doi:10.1016/j.bbailip.2021.158957.

Nelson, L.D., Johnson, A.E., & London, E. (2008). How interaction of perfringolysin O with membranes is controlled by sterol structure, lipid structure, and physiological low pH: Insights into the origin of perfringolysin O-lipid raft interaction. *The Journal of Biological Chemistry*, 283(8), 4632–4642. doi:10.1074/jbc.M709483200.

Nieves, D.J., & Owen, D.M. (2020). Quantitative mapping of membrane nanoenvironments through single-molecule imaging of solvatochromic probes. *bioRxiv*. doi:10.1101/2020.07.19.209908 %J.

Nishimura, S., Ishii, K., Iwamoto, K., Arita, Y., Matsunaga, S., & Ohno-Iwashita, Y., et al. (2013). Visualization of sterol-rich membrane domains with fluorescently-labeled theonellamides. *PLoS One*, 8(12), e83716. doi:10.1371/journal.pone.0083716.

Nizamov, S., Sednev, M.V., Bossi, M.L., Hebisch, E., Frauendorf, H., & Lehnart, S.E., et al. (2016). “Reduced” coumarin dyes with an O-phosphorylated 2,2-dimethyl-4-(hydroxymethyl)-1,2,3,4-tetrahydroquinoline fragment: Synthesis, spectra, and STED microscopy. *Chemistry – A European Journal*, 22(33), 11631–11642. doi:10.1002/chem.201601252.

Obaid, A.L., Loew, L.M., Wuskell, J.P., & Salzberg, B.M. (2004). Novel naphthylstyryl-pyridium potentiometric dyes offer advantages for neural network analysis. *Journal of Neuroscience Methods*, 134(2), 179–190. Retrieved from <http://www.ncbi.nlm.nih.gov/pubmed/15003384>.

Ohno-Iwashita, Y., Shimada, Y., Waheed, A.A., Hayashi, M., Inomata, M., & Nakamura, M., et al. (2004). Perfringolysin O, a cholesterol-binding cytolysin, as a probe for lipid rafts. *Anaerobe*, 10(2), 125–134. doi:10.1016/j.anaerobe.2003.09.003.

Orci, L., Montesano, R., Meda, P., Malaisse-Lagae, F., Brown, D., & Perrelet, A., et al. (1981). Heterogeneous distribution of filipin-cholesterol complexes across the cisternae of the Golgi apparatus. *Proceedings of the National Academy of Sciences of the United States of America*, 78, 293–297.

Pagac, M., Cooper, D.E., Qi, Y., Lukmantara, I.E., Mak, H.Y., & Wu, Z., et al. (2016). SEIPIN regulates lipid droplet expansion and adipocyte development by modulating the activity of glycerol-3-phosphate acyltransferase. *Cell Reports*, 17(6), 1546–1559. doi:10.1016/j.celrep.2016.10.037.

Parasassi, T., Conti, F., & Gratton, E. (1986). Time-resolved fluorescence emission spectra of Laurdan in phospholipid vesicles by multifrequency phase and modulation fluorometry. *Cellular and Molecular Biology*, 32(1), 103–108.

Parasassi, T., De Stasio, G., d’Ubaldo, A., & Gratton, E. (1990). Phase fluctuation in phospholipid membranes revealed by Laurdan fluorescence. *Biophysical Journal*, 57, 1179–1186.

Parasassi, T., De Stasio, G., Ravagnan, G., Rusch, R.M., & Gratton, E. (1991). Quantitation of lipid phases in phospholipid vesicles by the generalized polarization of Laurdan fluorescence. *Biophysical Journal*, 60, 179–189.

- Parasassi, T., Di Stefano, M., Ravagnan, G., Saporita, O., & Gratton, E. (1992). Membrane aging during cell growth ascertained by laurdan generalized polarization. *Experimental Cell Research*, 202, 432–439.
- Parasassi, T., & Gratton, E. (1992). Packing of phospholipid vesicles studied by oxygen quenching of Laurdan fluorescence. *Journal of Fluorescence*, 2, 167–174.
- Parasassi, T., Gratton, E., Yu, W.M., Wilson, P., & Levi, M. (1997). Two-photon fluorescence microscopy of Laurdan generalized polarization domains in model and natural membranes. *Biophysical Journal*, 72(6), 2413–2429.
- Parasassi, T., Krasnowska, E.K., Bagatolli, L., & Gratton, E. (1998). Laurdan and prodan as polarity-sensitive fluorescent membrane probes. *Journal of Fluorescence*, 8(4), 365–373. doi:10.1023/A:1020528716621.
- Parasassi, T., Loiero, M., Raimondi, M., Ravagnan, G., & Gratton, E. (1993a). Absence of lipid gel-phase domains in seven mammalian cell lines and in four primary cell types. *Biochimica Biophysica Acta Membrane*, 1153, 143–154.
- Parasassi, T., Loiero, M., Raimondi, M., Ravagnan, G., & Gratton, E. (1993b). Effect of cholesterol on phospholipid phase domains as detected by laurdan generalized polarization. *Biophysical Journal*, 64, A72.
- Parasassi, T., Ravagnan, G., Rusch, R.M., & Gratton, E. (1993). Modulation and dynamics of phase properties in phospholipid mixtures detected by Laurdan fluorescence. *Photochemistry and Photobiology*, 57, 403–410.
- Pentchev, P.G., Comly, M.E., Kruth, H.S., Vanier, M.T., Wenger, D.A., & Patel, S., et al. (1985). A defect in cholesterol esterification in Niemann-Pick disease (type C) patients. *Proceedings of the National Academy of Sciences of the United States of America*, 82(23), 8247–8251. doi:10.1073/pnas.82.23.8247.
- Radhakrishnan, A., Anderson, T.G., & McConnell, H.M. (2000). Condensed complexes, rafts, and the chemical activity of cholesterol in membranes. *Proceedings of the National Academy of Sciences of the United States of America*, 97(23), 12422–12427. Retrieved from <http://www.ncbi.nlm.nih.gov/pubmed/11050164>.
- Radhakrishnan, A., & McConnell, H.M. (1999). Cholesterol-phospholipid complexes in membranes. *Journal of the American Chemical Society*, 121(2), 486–487.
- Radhakrishnan, A., & McConnell, H.M. (2000). Chemical activity of cholesterol in membranes. *Biochemistry*, 39(28), 8119–8124. Retrieved from <http://www.ncbi.nlm.nih.gov/pubmed/0010889017>.
- Raghuraman, H., & Chattopadhyay, A. (2004). Influence of lipid chain unsaturation on membrane-bound melittin: A fluorescence approach. *Biochimica et Biophysica Acta*, 1665(1–2), 29–39. Retrieved from <http://www.ncbi.nlm.nih.gov/pubmed/15471568>.
- Ranjit, S., Malacrida, L., Jameson, D.M., & Gratton, E. (2018). Fit-free analysis of fluorescence lifetime imaging data using the phasor approach. *Nature Protocols*, 13(9), 1979–2004. doi:10.1038/s41596-018-0026-5.
- Robalo, J.R., do Canto, A.M., Carvalho, A.J., Ramalho, J.P., & Loura, L.M. (2013). Behavior of fluorescent cholesterol analogues dehydroergosterol and cholestatrienol in lipid bilayers: A molecular dynamics study. *The Journal of Physical Chemistry. B*, 117(19), 5806–5819. doi:10.1021/jp312026u.
- Ruggiero, A., & Hudson, B. (1989a). Analysis of the anisotropy decay of trans-parinaric acid in lipid bilayers. *Biophysical Journal*, 55, 1125–1135.

- Ruggiero, A., & Hudson, B. (1989b). Critical density fluctuations in lipid bilayers detected by fluorescence lifetime heterogeneity. *Biophysical Journal*, 55, 1111–1124.
- Saha, P., Shumate, J.L., Caldwell, J.G., Elghobashi-Meinhardt, N., Lu, A., & Zhang, L., et al. (2020). Inter-domain dynamics drive cholesterol transport by NPC1 and NPC1L1 proteins. *eLife*, 9. doi:10.7554/eLife.57089.
- Samsonov, A.V., Mihalyov, I., & Cohen, F.S. (2001). Characterization of cholesterol-sphingomyelin domains and their dynamics in bilayer membranes. *Biophysics Journal*, 81(3), 1486–1500. Retrieved from <http://www.ncbi.nlm.nih.gov/pubmed/11509362>.
- Sanchez, S.A., Tricceri, M.A., & Gratton, E. (2012). Laurdan generalized polarization fluctuations measures membrane packing micro-heterogeneity in vivo. *Proceedings of the National Academy of Sciences of the United States of America*, 109(19), 7314–7319. doi:10.1073/pnas.1118288109.
- Sanchez-Garcia, R., Segura, J., Maluenda, D., Carazo, J.M., & Sorzano, C.O.S. (2018). Deep Consensus, a deep learning-based approach for particle pruning in cryo-electron microscopy. *IUCrJ*, 5(Pt. 6), 854–865. doi:10.1107/S2052252518014392.
- Sander, C.L., Sears, A.E., Pinto, A.F.M., Choi, E.H., Kahremany, S., & Gao, F., et al. (2021). Nano-scale resolution of native retinal rod disk membranes reveals differences in lipid composition. *Journal of Cell Biology*, 220(8). doi:10.1083/jcb.202101063.
- Sato, S.B., Ishii, K., Makino, A., Iwabuchi, K., Yamaji-Hasegawa, A., & Senoh, Y., et al. (2004). Distribution and transport of cholesterol-rich membrane domains monitored by a membrane-impermeant fluorescent polyethylene glycol-derivatized cholesterol. *The Journal of Biological Chemistry*, 279(22), 23790–23796. Retrieved from <http://www.ncbi.nlm.nih.gov/pubmed/15026415>.
- Saunders, F.K., Mitchell, T.J., Walker, J.A., Andrew, P.W., & Boulnois, G.J. (1989). Pneumolysin, the thiol-activated toxin of *Streptococcus pneumoniae*, does not require a thiol group for in vitro activity. *Infection and Immunity*, 57(8), 2547–2552. doi:10.1128/iai.57.8.2547-2552.1989.
- Savinov, S.N., & Heuck, A.P. (2017). Interaction of cholesterol with perfringolysin O: What have we learned from functional analysis? *Toxins (Basel)*, 9(12). doi:10.3390/toxins9120381.
- Schroeder, F., Atshaves, B.P., Gallegos, A.M., McIntosh, A.L., Liu, J.C.S., & Kier, A.B., et al. (2005). Chapter 1 lipid rafts and caveolae organization. *Advances in Molecular and Cell Biology*, 36, 1–36. Elsevier.
- Schroeder, F., Myers-Payne, S.C., Billheimer, J.T., & Wood, W.G. (1995). Probing the ligand binding sites of fatty acid and sterol carrier proteins: Effects of ethanol. *Biochemistry*, 34(37), 11919–11927. Retrieved from <http://www.ncbi.nlm.nih.gov/pubmed/7547928>.
- Schueder, F., Strauss, M.T., Hoerl, D., Schnitzbauer, J., Schlichthaerle, T., & Strauss, S., et al. (2017). Universal super-resolution multiplexing by DNA exchange. *Angewandte Chemie (International Ed. in English)*, 56(14), 4052–4055. doi:10.1002/anie.201611729.
- Severs, N.J., & Robenek, H. (1983). Detection of microdomains in biomembranes. An appraisal of recent developments in freeze-fracture cytochemistry. *Biochimica et Biophysica Acta*, 737(3–4), 373–408. doi:10.1016/0304-4157(83)90007-2.
- Sezgin, E., Levental, I., Grzybek, M., Schwarzmann, G., Mueller, V., & Honigsmann, A., et al. (2012). Partitioning, diffusion, and ligand binding of raft lipid analogs in model and cellular plasma membranes. *Biochimica et Biophysica Acta*, 1818(7), 1777–1784. doi:10.1016/j.bbamem.2012.03.007.

- Sezgin, E., Levental, I., Mayor, S., & Eggeling, C. (2017). The mystery of membrane organization: Composition, regulation and roles of lipid rafts. *Nature Reviews. Molecular Cell Biology*. doi:10.1038/nrm.2017.16.
- Shaw, J.E., Epand, R.F., Epand, R.M., Li, Z., Bittman, R., & Yip, C.M. (2006). Correlated fluorescence-atomic force microscopy of membrane domains: Structure of fluorescence probes determines lipid localization. *Biophysical Journal*, 90(6), 2170–2178. Retrieved from <http://www.ncbi.nlm.nih.gov/pubmed/16361347>.
- Shcherbakova, D.M., Baloban, M., Emelyanov, A.V., Brenowitz, M., Guo, P., & Verkhusha, V.V. (2016). Bright monomeric near-infrared fluorescent proteins as tags and biosensors for multiscale imaging. *Nature Communications*, 7, 12405. doi:10.1038/ncomms12405.
- Shinitzky, M., Dianoux, A.C., Gitler, C., & Weber, G. (1971). Microviscosity and order in the hydrocarbon region of micelles and membranes determined with fluorescent probes. I. Synthetic micelles. *Biochemistry*, 10(11), 2106–2113. doi:10.1021/bi00787a023.
- Shinitzky, M., & Inbar, M. (1976). Microviscosity parameters and protein mobility in biological membranes. *Biochimica et Biophysica Acta*, 433, 133–149.
- Simons, K., & Ikonen, E. (1997). Functional rafts in cell membranes. *Nature*, 387(6633), 569–572. Retrieved from <http://www.ncbi.nlm.nih.gov/pubmed/9177342>.
- Solanko, K.A., Modzel, M., Solanko, L.M., & Wüstner, D. (2015). Fluorescent sterols and cholesteryl esters as probes for intracellular cholesterol transport. *Lipid Insights*, 8(Suppl. 1), 95–114. doi:10.4137/lpi.S31617.
- St. Clair, J.W., Kakuda, S., & London, E. (2020). Induction of ordered lipid raft domain formation by loss of lipid asymmetry. *Biophysical Journal*, 119(3), 483–492. <https://doi.org/10.1016/j.bpj.2020.06.030>.
- St. Clair, J.W., & London, E. (2019). Effect of sterol structure on ordered membrane domain (raft) stability in symmetric and asymmetric vesicles. *Biochimica et Biophysica Acta - Biomembranes*, 1861(6), 1112–1122. doi:10.1016/j.bbamem.2019.03.012.
- Steck, T.L., & Lange, Y. (2018). Transverse distribution of plasma membrane bilayer cholesterol: Picking sides. *Traffic*, 19(10), 750–760. doi:10.1111/tra.12586.
- Stolowich, N.J., Frolov, A., Atshaves, B., Murphy, E.J., Jolly, C.A., & Billheimer, J.T., et al. (1997). The sterol carrier protein-2 fatty acid binding site: An NMR, circular dichroic, and fluorescence spectroscopic determination. *The Biochemist*, 36(7), 1719–1729.
- Tangorra, A., Ferretti, G., Zolese, G., & Curatola, G. (1994). Study of plasma membrane heterogeneity using a phosphatidylcholine derivative of 1,6-diphenyl-1,3,5-hexatriene [2-(3-(diphenylhexatriene)propanoyl)-3-palmitoyl-L- $\alpha$ -phosphatidylcholine]. *Journal of Fluorescence*, 4(4), 357–360. doi:10.1007/bf01881456.
- Teo, A.C.K., Lee, S.C., Pollock, N.L., Stroud, Z., Hall, S., & Thakker, A., et al. (2019). Analysis of SMALP co-extracted phospholipids shows distinct membrane environments for three classes of bacterial membrane protein. *Scientific Reports*, 9(1), 1813. doi:10.1038/s41598-018-37962-0.
- Tory, M.C., & Merrill, A.R. (2002). Determination of membrane protein topology by red-edge excitation shift analysis: Application to the membrane-bound colicin E1 channel peptide. *Biochimica et Biophysica Acta*, 1564(2), 435–448. doi:10.1016/s0005-2736(02)00493-5.
- Tosheva, K.L., Yuan, Y., Matos Pereira, P., Culley, S., & Henriques, R. (2020). Between life and death: Strategies to reduce phototoxicity in super-resolution microscopy. *Journal of Physics D: Applied Physics*,

Truong, L., & Ferré-D'Amaré, A.R. (2019). From fluorescent proteins to fluorogenic RNAs: Tools for imaging cellular macromolecules. *Protein Science*, 28(8), 1374–1386. doi:10.1002/pro.3632.

Tsuji, T., Cheng, J., Tatematsu, T., Ebata, A., Kamikawa, H., & Fujita, A., et al. (2019). Predominant localization of phosphatidylserine at the cytoplasmic leaflet of the ER, and its TMEM16K-dependent redistribution. *Proceedings of the National Academy of Sciences of the United States of America*, 116(27), 13368–13373. doi:10.1073/pnas.1822025116.

Tweten, R.K. (1988). Cloning and expression in *Escherichia coli* of the perfringolysin O (theta-toxin) gene from *Clostridium perfringens* and characterization of the gene product. *Infection and Immunity*, 56(12), 3228–3234. doi:10.1128/iai.56.12.3228-3234.1988.

Uchida, Y., Hasegawa, J., Chinnapen, D., Inoue, T., Okazaki, S., & Kato, R., et al. (2011). Intracellular phosphatidylserine is essential for retrograde membrane traffic through endosomes. *Proceedings of the National Academy of Sciences of the United States of America*, 108(38), 15846–15851. doi:10.1073/pnas.1109101108.

Urbani, L., & Simoni, R.D. (1990). Cholesterol and vesicular stomatitis virus G protein take separate routes from the endoplasmic reticulum to the plasma membrane. *The Journal of Biological Chemistry*, 265(4), 1919–1923.

van de Linde, S., Heilemann, M., & Sauer, M. (2012). Live-cell super-resolution imaging with synthetic fluorophores. *Annual Review of Physical Chemistry*, 63, 519–540. doi:10.1146/annurev-physchem-032811-112012.

van der Velde, J., Smit, J., Punter, M., & Cordes, T. (2018). Self-healing dyes for super-resolution microscopy. *bioRxiv*. doi:10.1101/373852.

van Meer, G. (2011). Dynamic transbilayer lipid asymmetry. *Cold Spring Harbor Perspectives in Biology*, 3(5). doi:10.1101/cshperspect.a004671.

van Meer, G., Voelker, D.R., & Feigenson, G.W. (2008). Membrane lipids: Where they are and how they behave. *Nature Reviews. Molecular Cell Biology*, 9(2), 112–124. Retrieved from <http://www.ncbi.nlm.nih.gov/pubmed/18216768>.

van Wee, R., Filius, M., & Joo, C. (2021). Completing the canvas: Advances and challenges for DNA-PAINT super-resolution imaging. *Trends in Biochemical Sciences*. <https://doi.org/10.1016/j.tibs.2021.05.010>.

Varnai, P., & Balla, T. (1998). Visualization of phosphoinositides that bind pleckstrin homology domains: Calcium- and agonist-induced dynamic changes and relationship to myo-[<sup>3</sup>H]inositol-labeled phosphoinositide pools. *The Journal of Cell Biology*, 143(2), 501–510. Retrieved from <http://www.ncbi.nlm.nih.gov/pubmed/9786958>.

Veatch, S.L., & Keller, S.L. (2002). Organization in lipid membranes containing cholesterol. *Physical Review Letters*, 89(26), 268101. Retrieved from <http://www.ncbi.nlm.nih.gov/pubmed/12484857>.

Veatch, S.L., & Keller, S.L. (2003a). A closer look at the canonical “Raft Mixture” in model membrane studies. *Biophysical Journal*, 84(1), 725–726. Retrieved from <http://www.ncbi.nlm.nih.gov/pubmed/12524324>.

Veatch, S.L., & Keller, S.L. (2003b). Separation of liquid phases in giant vesicles of ternary mixtures of phospholipids and cholesterol. *Biophysical Journal*, 85(5), 3074–3083. Retrieved from <http://www.ncbi.nlm.nih.gov/pubmed/12524324>.

Veatch, S.L., & Keller, S.L. (2005). Seeing spots: Complex phase behavior in simple membranes. *Biochimica et Biophysica Acta*, 1746(3), 172–185. Retrieved from <http://www.ncbi.nlm.nih.gov/pubmed/16043244>.

Wade, O.K., Woehrstein, J.B., Nickels, P.C., Strauss, S., Stehr, F., & Stein, J., et al. (2019). 124-Color super-resolution imaging by engineering DNA-PAINT blinking kinetics. *Nano Letters*, 19(4), 2641–2646. doi:10.1021/acs.nanolett.9b00508.

Waheed, A.A., Shimada, Y., Heijnen, H.F., Nakamura, M., Inomata, M., & Hayashi, M., et al. (2001). Selective binding of perfringolysin O derivative to cholesterol-rich membrane microdomains (rafts). *Proceedings of the National Academy of Sciences of the United States of America*, 98(9), 4926–4931. doi:10.1073/pnas.091090798.

Weber, G. (1952). Polarization of the fluorescence of macromolecules. II. Fluorescent conjugates of ovalbumin and bovine serum albumin. *Biochemical Journal*, 51(2), 155–167. doi:10.1042/bj0510155.

Weber, G., & Farris, F.J. (1979). Synthesis and spectral properties of a hydrophobic fluorescent probe: 6-Propionyl-2-(dimethylamino)naphthalene. *Biochemistry*, 18(14), 3075–3078.

Weber, M., Khan, T.A., Patalag, L.J., Bossi, M., Leutenegger, M., & Belov, V.N., et al. (2021). Photoactivatable fluorophore for stimulated emission depletion (STED) microscopy and bioconjugation technique for hydrophobic labels. *Chemistry*, 27(1), 451–458. doi:10.1002/chem.202004645.

Weber, G., & Laurence, D.J. (1954). Fluorescent indicators of adsorption in aqueous solution and on the solid phase. *The Biochemical Journal*, 56(325th Meeting), xxxi.

Wenz, J.J., & Barrantes, F.J. (2003). Steroid structural requirements for stabilizing or disrupting lipid domains. *Biochemistry*, 42(48), 14267–14276. doi:10.1021/bi035759c.

Wharton, S.A., De Martinez, S.G., & Green, C. (1980). Use of fluorescent probes in the study of phospholipid—sterol bilayers. *The Biochemical Journal*, 191(3), 785–790. doi:10.1042/bj1910785.

Wildanger, D., Rittweger, E., Kastrop, L., & Hell, S.W. (2008). STED microscopy with a supercontinuum laser source. *Optics Express*, 16(13), 9614–9621. Retrieved from <http://www.ncbi.nlm.nih.gov/pubmed/18575529>.

Wilhelm, L.P., Voilquin, L., Kobayashi, T., Tomasetto, C., & Alpy, F. (2019). Intracellular and plasma membrane cholesterol labeling and quantification using filipin and GFP-D4. *Methods in Molecular Biology*, 1949, 137–152. doi:10.1007/978-1-4939-9136-5\_11.

Wüstner, D. (2007). Plasma membrane sterol distribution resembles the surface topography of living cells. *Molecular Biology of the Cell*, 18(1), 211–228. Retrieved from <http://www.ncbi.nlm.nih.gov/pubmed/17065557>.

Wüstner, D., Herrmann, A., Hao, M., & Maxfield, F.R. (2002). Rapid nonvesicular transport of sterol between the plasma membrane domains of polarized hepatic cells. *The Journal of Biological Chemistry*, 277(33), 30325–30336. Retrieved from <http://www.ncbi.nlm.nih.gov/pubmed/12050151>.

Xu, R., Xu, Y., Wang, Z., Zhou, Y., Dang, D., & Meng, L. (2020). Recent advances on organic fluorescent probes for stimulated emission depletion (STED) microscopy. *Combinatorial Chemistry & High Throughput Screening*. doi:10.2174/1386207323666200917104203.



Yamamura, K., Ashida, H., Okano, T., Kinoshita-Daitoku, R., Suzuki, S., & Ohtani, K., et al. (2019). Inflammasome activation induced by perfringolysin O of *Clostridium perfringens* and its involvement in the progression of gas gangrene. *Frontiers in Microbiology*, 10, 2406. doi:10.3389/fmicb.2019.02406.

Yeagle, P.L. (1989). Lipid regulation of cell membrane structure and function. *The FASEB Journal*, 3, 1833–1842.


Yeung, T., Gilbert, G.E., Shi, J., Silvius, J., Kapus, A., & Grinstein, S. (2008). Membrane phosphatidylserine regulates surface charge and protein localization. *Science*, 319(5860), 210–213. doi:10.1126/science.1152066.

Yokoyama, Y., Terada, T., Shimizu, K., Nishikawa, K., Kozai, D., & Shimada, A., et al. (2020). Development of a deep learning-based method to identify “good” regions of a cryo-electron microscopy grid. *Biophysical Reviews*, 12(2), 349–354. doi:10.1007/s12551-020-00669-6.

Yu, D., Gustafson, W.C., Han, C., Lafaye, C., Noirclerc-Savoie, M., & Ge, W.P., et al. (2014). An improved monomeric infrared fluorescent protein for neuronal and tumour brain imaging. *Nature Communications*, 5, 3626. doi:10.1038/ncomms4626.

Zhang, Z., Kenny, S.J., Hauser, M., Li, W., & Xu, K. (2015). Ultrahigh-throughput single-molecule spectroscopy and spectrally resolved super-resolution microscopy. *Nature Methods*, 12(10), 935–938. doi:10.1038/nmeth.3528.

## **Q7** Further reading

 The corrections made in this section will be reviewed and approved by a journal production editor. The newly added/removed references and its citations will be reordered and rearranged by the production team.

McNicholas, S., Potterton, E., Wilson, K.S., & Noble, M.E. (2011). Presenting your structures: The CCP4mg molecular-graphics software. *Acta Crystallographica. Section D, Biological Crystallography*, 67(Pt 4), 386–394. doi:10.1107/s0907444911007281.

**Keywords:** Fluorescence microscopy; Sensors; Biosensors; Cholesterol; Membrane domains; Fluorescent probes; Super-resolution microscopy; Nanoscopy; Transbilayer distribution; In-plane distribution; Lipid domain; Lipid asymmetry; Virtual staining

## Queries and Answers

**Q1**

**Query:** Please note that "Francisco J." has been treated as initial and "Barrantes" has been treated as surname in the author name "Francisco J. Barrantes". Please check and confirm if it is correct.

**Answer:** correct

Q2

**Query:** Please provide appropriate chapter title followed by author names in place of "Chapter 6" mentioned here.

**Answer:** This should be provided by the Editors

Q3

**Query:** Please provide appropriate chapter title followed by author names in place of "Chapter 10" mentioned here and in subsequent occurrences.

**Answer:** This should be provided by the Editors

Q4

**Query:** The citation "Naito & Saheki, 2021" has been changed to "Naito & Saheki, 1866" to match the author name/date in the reference list. Please check if the change is fine in this occurrence and modify the subsequent occurrences, if necessary.

**Answer:** This is wrong. It's Naito & Saheki, 2021.

1866 is the volume. The reference is as follows:

Biochim Biophys Acta Mol Cell Biol Lipids. 2021 Aug;1866(8):158957. doi: 10.1016/j.bbalip.2021.158957.

Q5

**Query:** Please provide appropriate chapter title followed by author names in place of "Chapter 7" mentioned here.

**Answer:** The Editors should know this.

Q6

**Query:** Please check whether the volume number and page number are appropriate as inserted for reference "Buwaneka et al., 202.

**Answer:** yes, thank you

Q7

**Query:** Further reading section contains references that are not cited in manuscript text. Please cite the references or confirm if we could delete it? Further reading will be retained if the references are not cited or deleted.

**Answer:** This reference corresponds to the author of the molecular graphics software used in Figure 4. It is quoted in the legend to Figure 4. PLEASE INCORPORATE IT IN THE REFERENCE LIST.